Examples of X-ray characterization techniques in energy storage research

Katharine L. Harrison (National Renewable Energy Lab)

Many coauthors acknowledged throughout

Denver X-ray Conference

S-16 Energy Materials Characterization Session

08/09/2024 8:30-9:00 am

katie.harrison@nrel.gov

Outline

Introduction to rechargeable Li batteries

Example 1: understanding substitution and doping in $LiFePO_4$ cathode materials using X-ray and other characterization techniques

Example 2: understanding stress in Li metal anodes using X-ray techniques

Importance of rechargeable Li-ion batteries

Electric vehicles and portable electronics

Rapid growth in sales expected

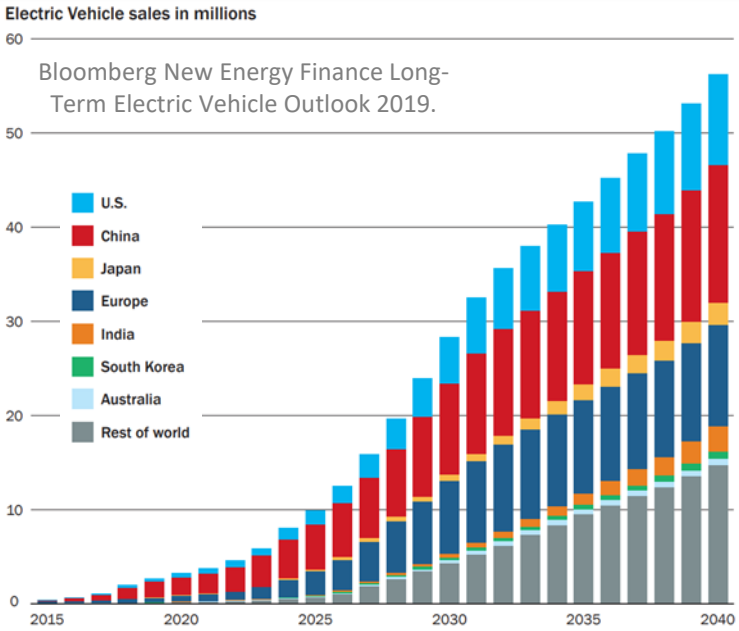

Bloomberg New Energy Finance Long-Term Electric Vehicle Outlook 2019.

Rapid growth in research publications

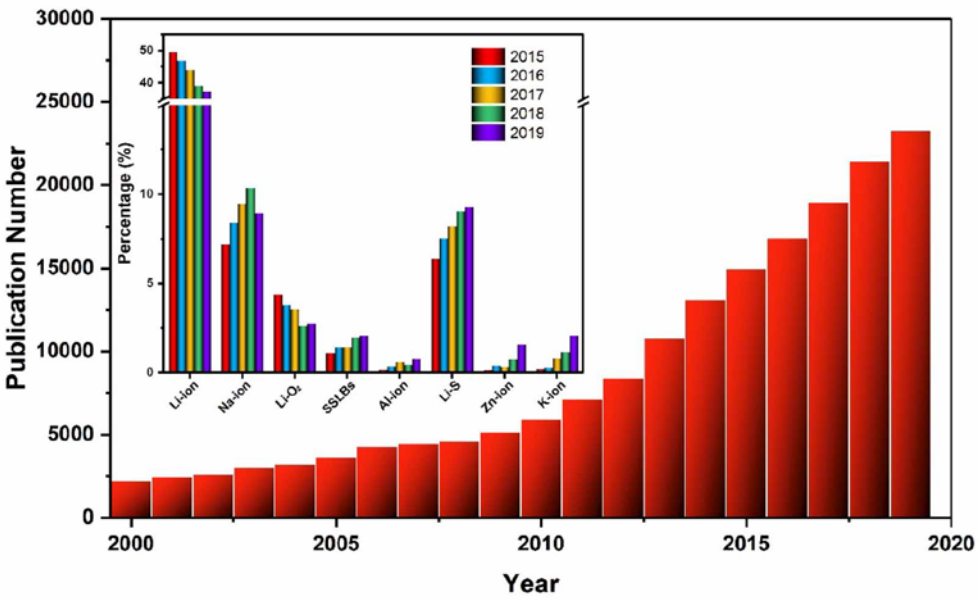

Ma, J., Li, Y., Grundish, N.S., Goodenough, J.B., Chen, Y., Guo, L., Peng, Z., Qi, X., Yang, F., Qie, L. and Wang, C.A., 2021. The 2021 battery technology roadmap. *Journal of Physics D: Applied Physics*, *54*(18), p.183001.

Li-ion battery materials basics and materials research areas

Li-ion battery during discharge

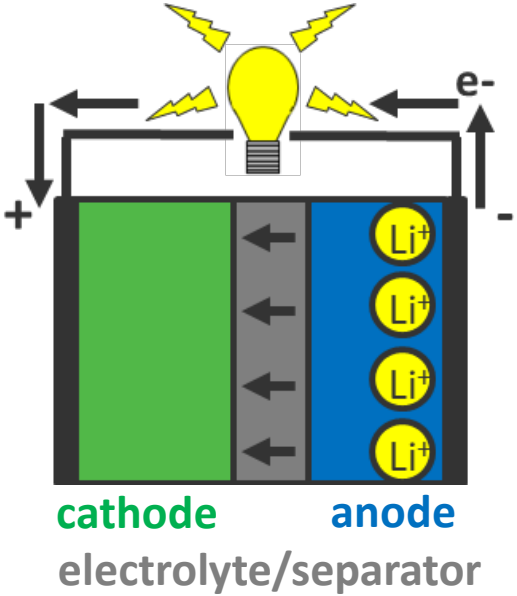

Li-ion battery materials basics and materials research areas

State of the Art Insertion Cathodes

$LiCoO_2$ $LiFePO_4$ $LiMn_2O_4$
$LiNi_xMn_yCo_{1-x-y}O_2$
$LiNi_xCo_yAl_{1-x-y}O_2$

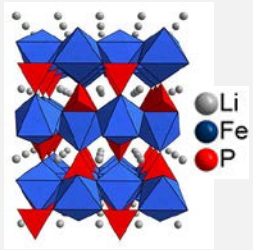

Alternative Cathode Research

Insertion

$Li_3V_2(PO_4)_3$
$LiVOPO_4$

Conversion

FeF_3
Oxygen
Sulfur

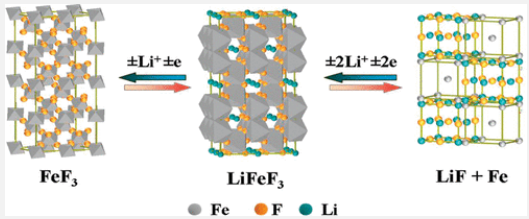

Li-ion battery during discharge

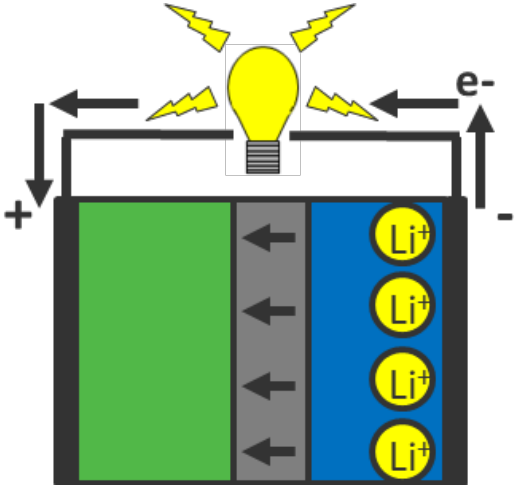

Molenda, J. and Molenda, M., 2011. *Composite cathode material for Li-Ion batteries based on $ LiFePO_4 $ system*. Rijeka: InTech.
Li, T., Li, L., Cao, Y.L., Ai, X.P. and Yang, H.X., 2010. Reversible three-electron redox behaviors of FeF3 nanocrystals as high-capacity cathode-active materials for Li-ion batteries. *The Journal of Physical Chemistry C*, *114*(7), pp.3190-3195.

Li-ion battery materials basics and materials research areas

State of the Art Insertion Cathodes

$LiCoO_2$ $LiFePO_4$ $LiMn_2O_4$
$LiNi_xMn_yCo_{1-x-y}O_2$
$LiNi_xCo_yAl_{1-x-y}O_2$

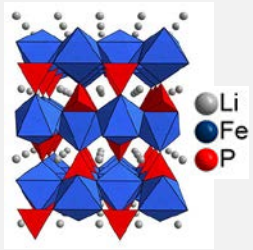

Alternative Cathode Research

Insertion

$Li_3V_2(PO_4)_3$
$LiVOPO_4$

Conversion

FeF_3
Oxygen
Sulfur

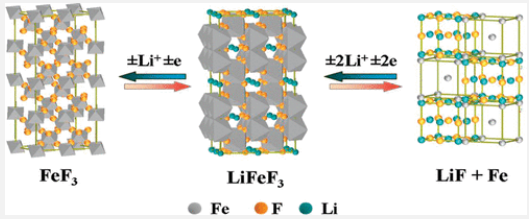

Li-ion battery during discharge

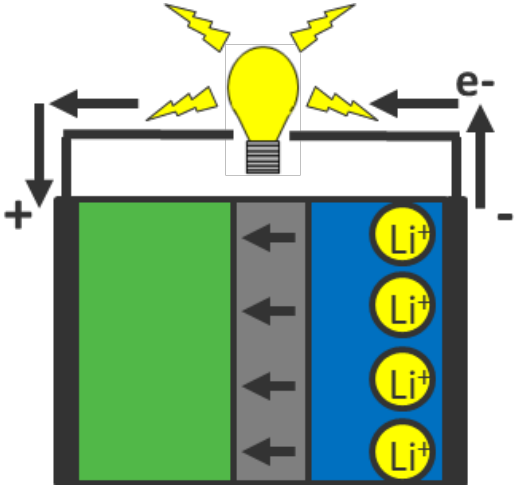

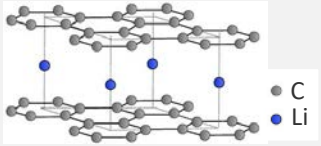

State of the Art Insertion Anodes

Graphite
$Li_4Ti_5O_{12}$

Alternative Anode Research

Alloys

Si, Sn

Carbons

graphene

Metal

Li

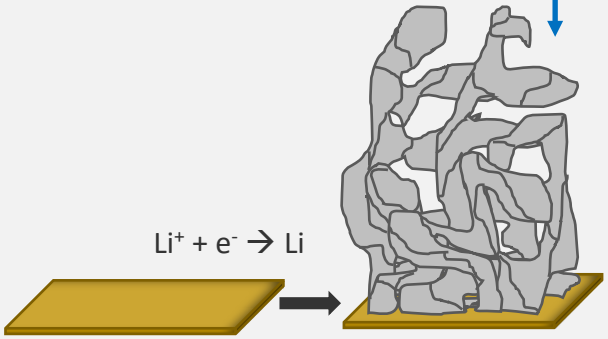

Molenda, J. and Molenda, M., 2011. *Composite cathode material for Li-Ion batteries based on $ LiFePO_4 $ system*. Rijeka: InTech.
Li, T., Li, L., Cao, Y.L., Ai, X.P. and Yang, H.X., 2010. Reversible three-electron redox behaviors of FeF3 nanocrystals as high-capacity cathode-active materials for Li-ion batteries. *The Journal of Physical Chemistry C*, *114*(7), pp.3190-3195.
Pistorio, F., Clerici, D., Mocera, F. and Somà, A., 2022. Review on the experimental characterization of fracture in active material for lithium-ion batteries. *Energies*, *15*(23), p.9168.

Li-ion battery materials basics and materials research areas

State of the Art Insertion Cathodes

$LiCoO_2$ **$LiFePO_4$** $LiMn_2O_4$

$LiNi_xMn_yCo_{1-x-y}O_2$

$LiNi_xCo_yAl_{1-x-y}O_2$

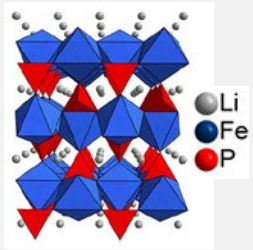

Alternative Cathode Research

Insertion

$Li_3V_2(PO_4)_3$

$LiVOPO_4$

Conversion

FeF_3

Oxygen

Sulfur

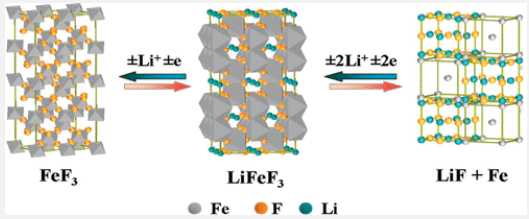

Li-ion battery during discharge

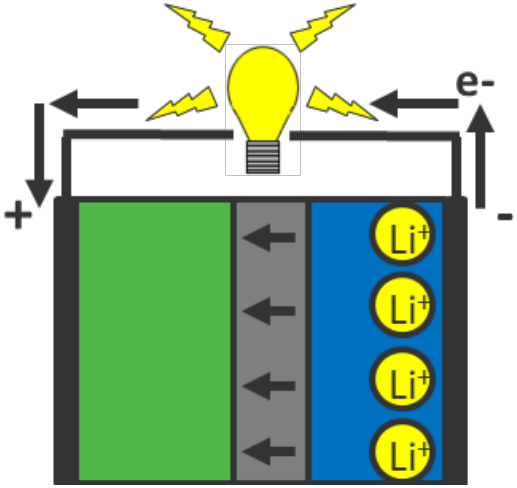

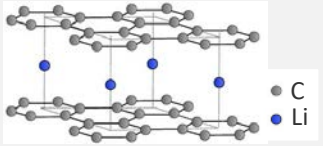

State of the Art Insertion Anodes

Graphite

$Li_4Ti_5O_{12}$

Alternative Anode Research

Alloys

Si, Sn

Carbons

graphene

Metal

Li

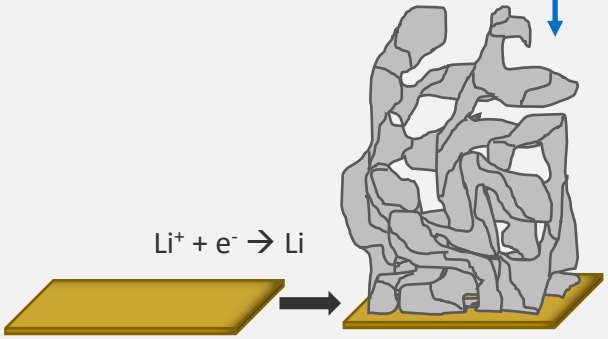

Molenda, J. and Molenda, M., 2011. *Composite cathode material for Li-Ion batteries based on $ LiFePO_4 $ system*. Rijeka: InTech.

Li, T., Li, L., Cao, Y.L., Ai, X.P. and Yang, H.X., 2010. Reversible three-electron redox behaviors of FeF3 nanocrystals as high-capacity cathode-active materials for Li-ion batteries. *The Journal of Physical Chemistry C*, *114*(7), pp.3190-3195.

Pistorio, F., Clerici, D., Mocera, F. and Somà, A., 2022. Review on the experimental characterization of fracture in active material for lithium-ion batteries. *Energies*, *15*(23), p.9168.

Outline

Introduction to rechargeable Li batteries

Example 1: understanding substitution and doping in $LiFePO_4$ cathode materials using X-ray and other characterization techniques

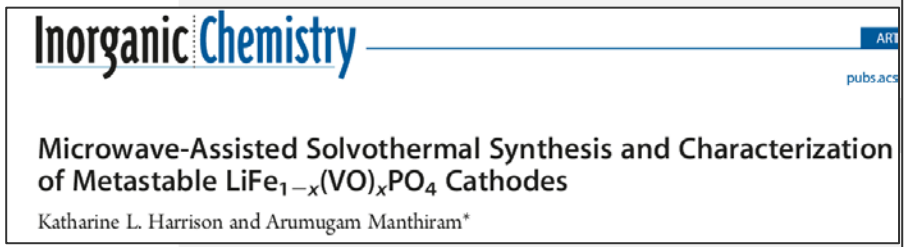
Inorganic Chemistry

ART

pubs.acs

Microwave-Assisted Solvothermal Synthesis and Characterization of Metastable $LiFe_{1-x}(VO)_xPO_4$ Cathodes

Katharine L. Harrison and Arumugam Manthiram*

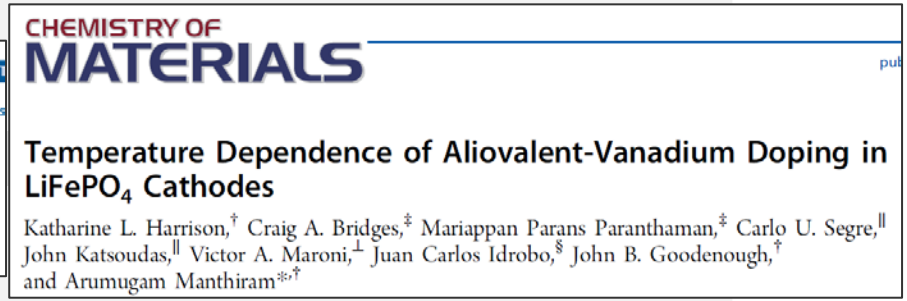
CHEMISTRY OF MATERIALS

pub

Temperature Dependence of Aliovalent-Vanadium Doping in $LiFePO_4$ Cathodes

Katharine L. Harrison,† Craig A. Bridges,‡ Mariappan Parans Paranthaman,‡ Carlo U. Segre,‖ John Katsoudas,‖ Victor A. Maroni,⊥ Juan Carlos Idrobo,§ John B. Goodenough,† and Arumugam Manthiram*,†

Project motivation

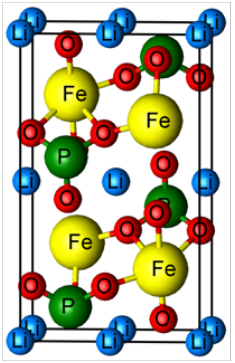

$LiFePO_4$

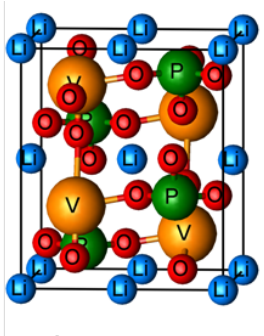

β-$LiVOPO_4$

Cathode	Space Group	Potential	Capacity
$LiFePO_4$	*Pnma*	3.45 V	170 mAh/g
β-$LiVOPO_4$	*Pnma*	4.0 V	159 mAh/g

$LiFePO_4$ safe and inexpensive cathode but low electronic conductivity and energy density.

Improve energy density of $LiFePO_4$ by substituting some $(VO)^{2+}$ for Fe^{2+}.

Same space group but different structures, so unclear if substitution possible.

Low temperature synthesis may enable metastable phase if thermodynamically unstable.

Harrison and Manthiram, 2011. *Inorganic chemistry*, *50*(8), pp.3613-3620.

Low temperature microwave-assisted solvothermal (MW-ST) synthesis as a green manufacturing approach and platform for enabling metastable phases

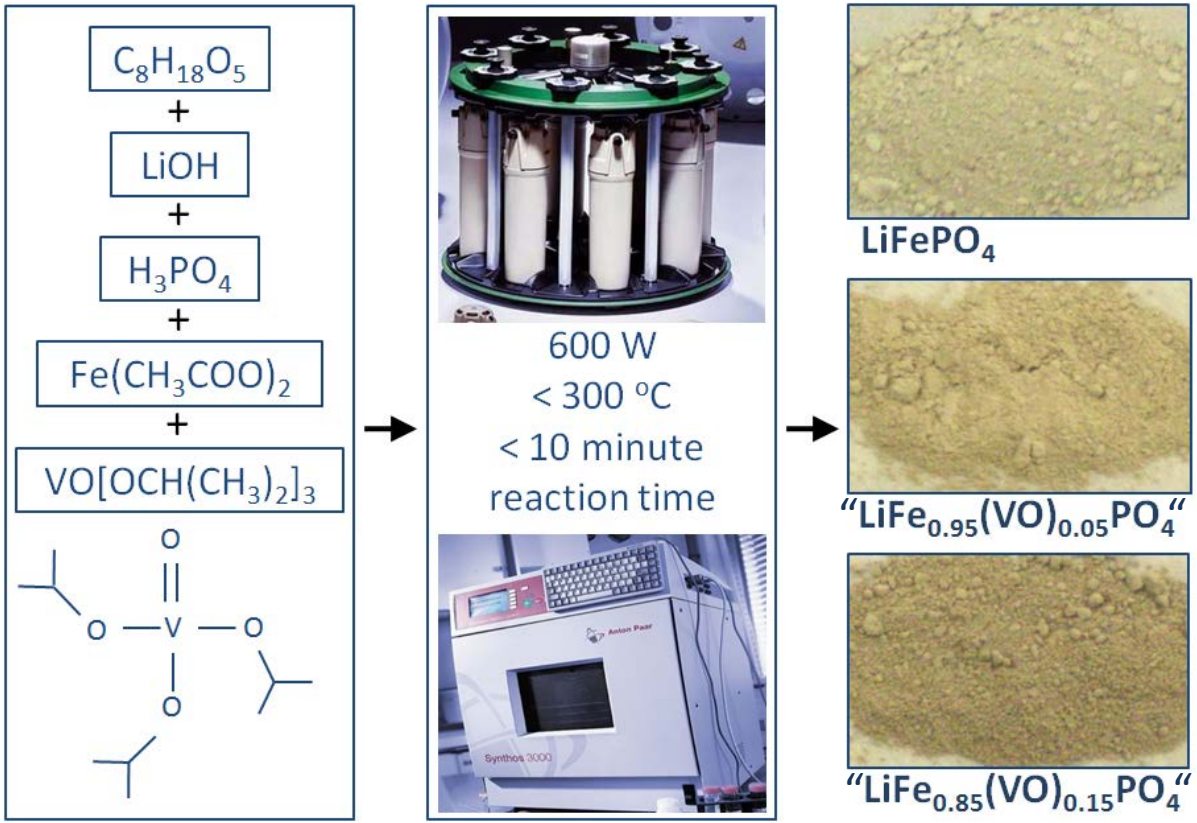

Harrison and Manthiram, 2011. *Inorganic chemistry*, *50*(8), pp.3613-3620.

X-ray diffraction shows a systematic decrease in unit cell volume with increases in $(VO)^{2+}$ addition

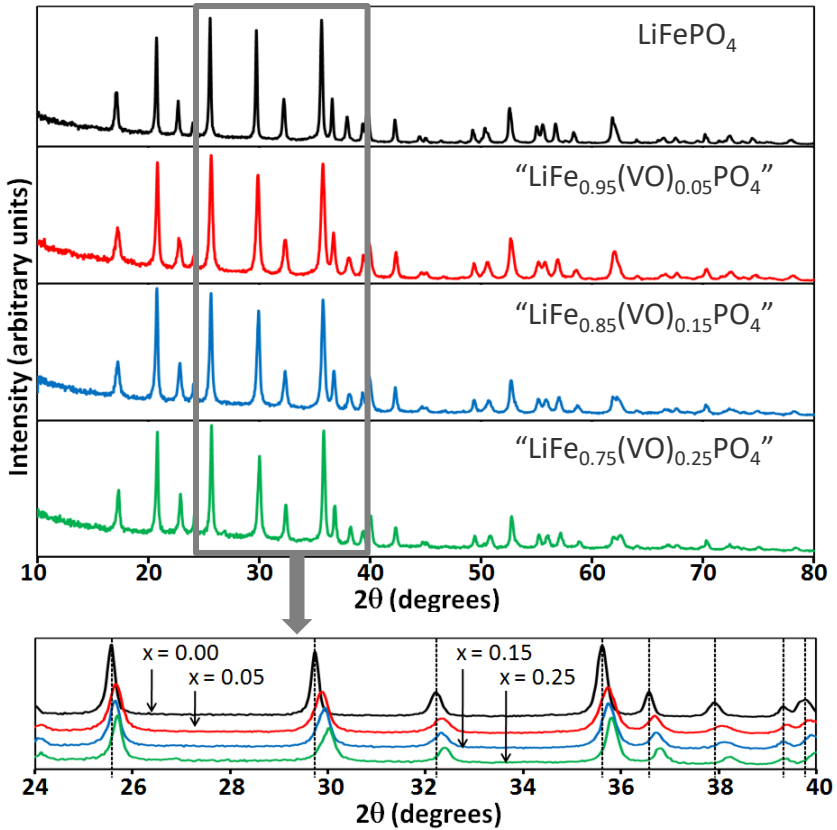

Sample	Volume (Å^3)	Li/P	V/P	Fe/P
$LiFePO_4$	290.34	1.00	-----	0.99
"$LiFe_{0.95}(VO)_{0.05}PO_4$"	289.59	0.99	0.05	0.96
"$LiFe_{0.90}(VO)_{0.10}PO_4$"	288.66	0.97	0.10	0.86
"$LiFe_{0.85}(VO)_{0.15}PO_4$"	287.96	1.02	0.16	0.77
"$LiFe_{0.75}(VO)_{0.25}PO_4$"	286.92	0.99	0.24	0.70

Volume decreases with increasing $(VO)^{2+}$, despite $(VO)^{2+}$ being larger than Fe^{2+}.

Fe_3O_4 impurity formed (and removed) with stoichiometric $(VO)^{2+}$ substitution for Fe^{2+} and ICP shows Fe/P lower than expected.

Theorized that Fe^{2+} vacancies form to allow space for $(VO)^{2+}$, compensated by Fe^{3+}.

Harrison and Manthiram, 2011. *Inorganic chemistry*, *50*(8), pp.3613-3620.

ICP = inductively coupled plasma

FTIR shows shoulder grows with increasing $(VO)^{2+}$ content, consistent with $(VO)^{2+}$ substitution

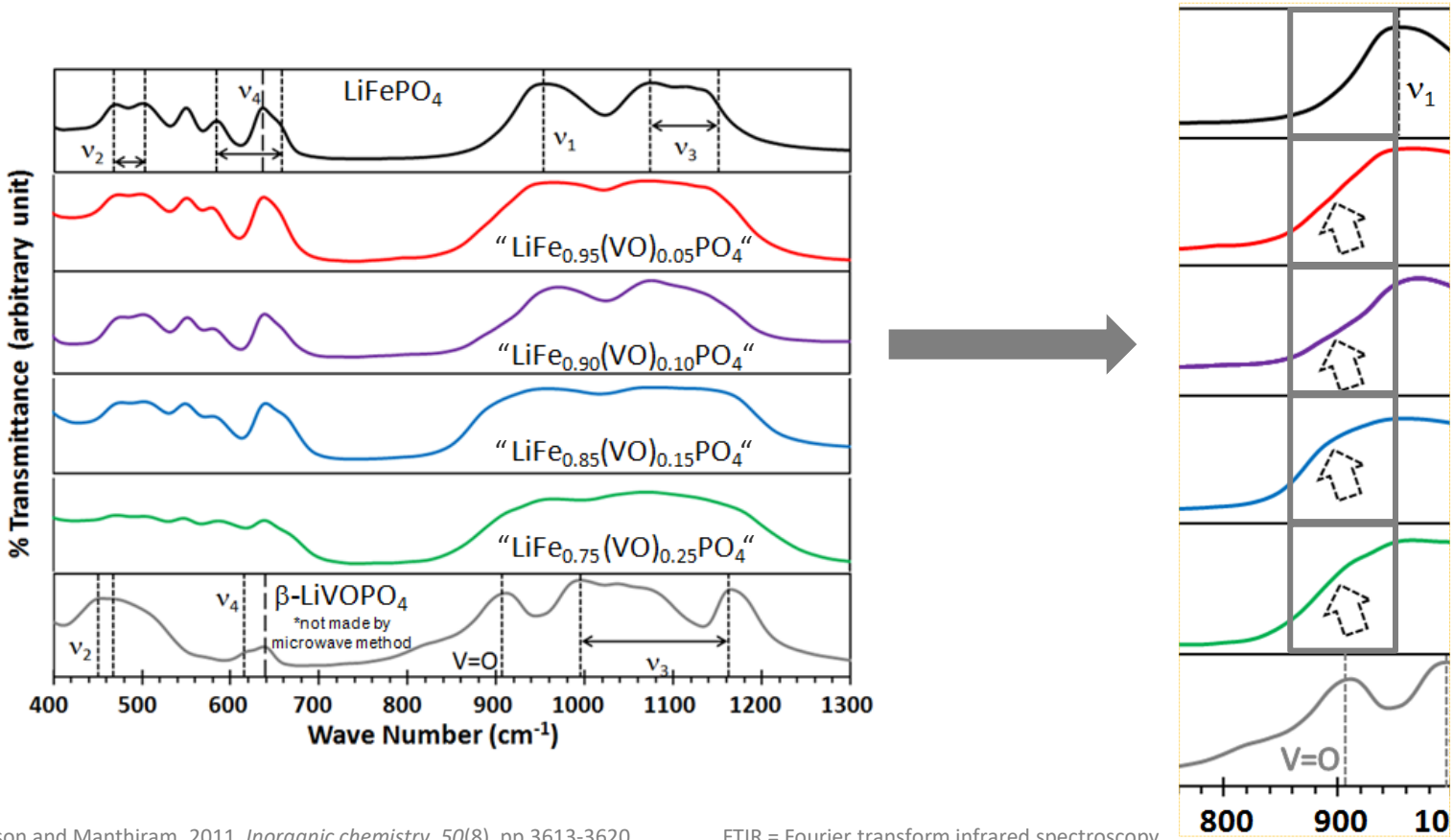

Harrison and Manthiram, 2011. *Inorganic chemistry*, *50*(8), pp.3613-3620.

FTIR = Fourier transform infrared spectroscopy

V 2p XPS suggests V^{4+}, consistent with $(VO)^{2+}$

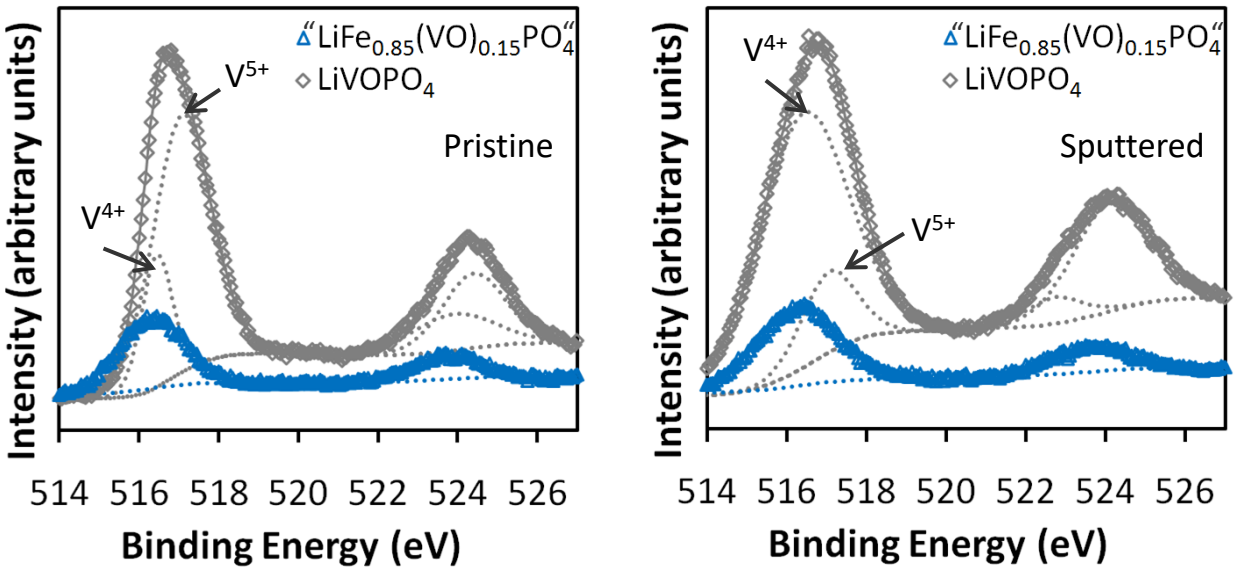

- $LiVOPO_4$ shows V^{4+} and V^{5+} even after sputtering.
- Fe spectra for $LiFePO_4$ and $LiFe_{0.85}(VO)_{0.15}PO_4$ show mixed Fe^{2+} and Fe^{3+}.
- XPS is a surface technique and not ideal for bulk oxidation state analysis.

Harrison and Manthiram, 2011. *Inorganic chemistry*, *50*(8), pp.3613-3620.

XPS = X-ray photoelectron spectroscopy

Galvanostatic cycling

C/10 = 10 h discharge
C/2 = 2 h discharge
2C = ½ discharge

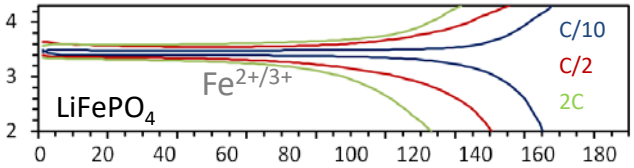

Voltage (V)

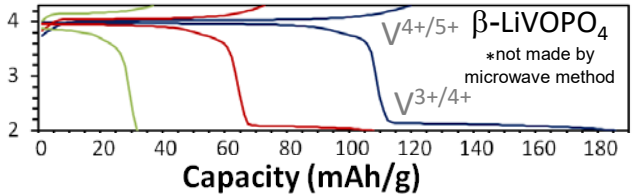

Harrison and Manthiram, 2011. *Inorganic chemistry*, *50*(8), pp.3613-3620.

Galvanostatic cycling

$V^{4+/5+}$ appears redox active

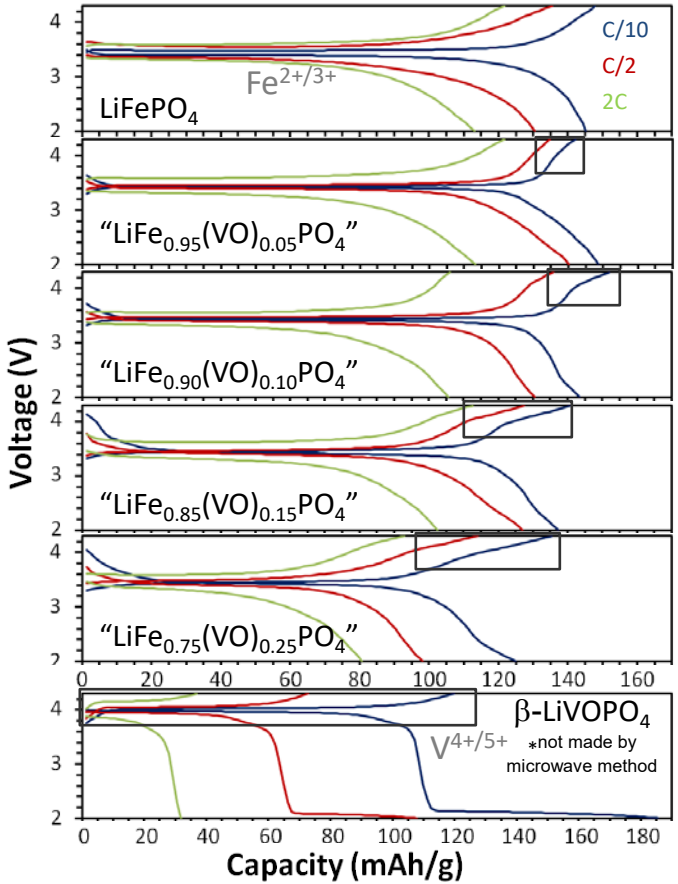

Harrison and Manthiram, 2011. *Inorganic chemistry*, *50*(8), pp.3613-3620.

Galvanostatic cycling

$V^{4+/5+}$ appears redox active

$V^{3+/4+}$ appears redox active

C/10 = 10 h discharge
C/2 = 2 h discharge
2C = ½ discharge

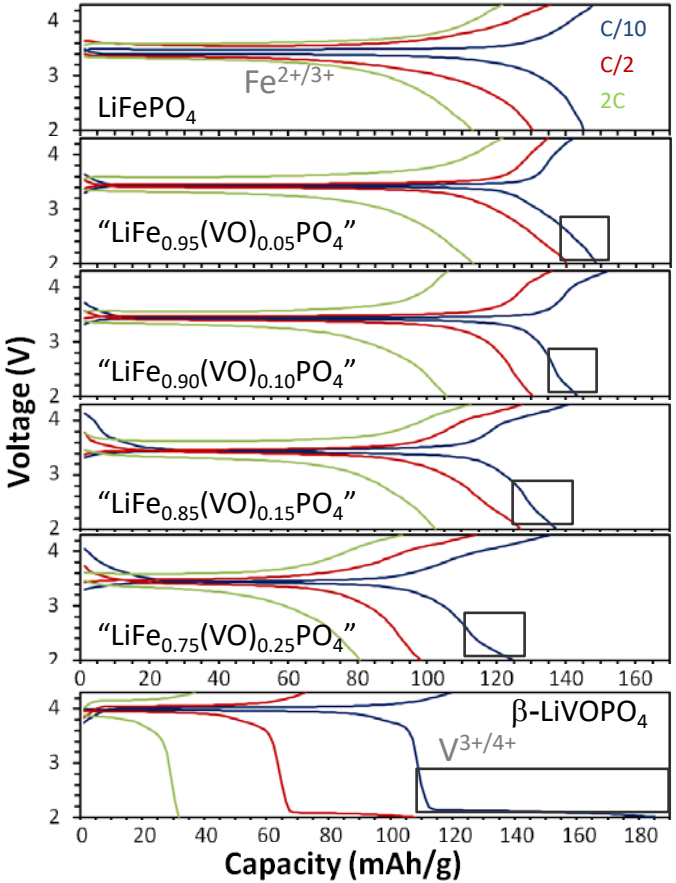

Harrison and Manthiram, 2011. *Inorganic chemistry*, *50*(8), pp.3613-3620.

Is $(VO)^{2+}$ substituted for Fe^{2+} or is V^{x+} doped into $LiFePO_4$, potentially leading to distorted VO_6?

Synthesized "$LiFe_{1-x}(VO)_xPO_4$" with $0 \leq x \leq 0.25$ by a microwave-solvothermal process (<300 °C).

XRD suggests systematic substitution into crystal lattice, FTIR/electrochemistry consistent with $(VO)^{2+}$.

Harrison and Manthiram, 2011. *Inorganic chemistry*, *50*(8), pp.3613-3620.

Is $(VO)^{2+}$ substituted for Fe^{2+} or is V^{x+} doped into $LiFePO_4$, potentially leading to distorted VO_6?

Synthesized "$LiFe_{1-x}(VO)_xPO_4$" with $0 \leq x \leq 0.25$ by a microwave-solvothermal process (<300 °C).

XRD suggests systematic substitution into crystal lattice, FTIR/electrochemistry consistent with $(VO)^{2+}$.

Fe_3O_4 impurity forms and ICP suggests iron vacancies in lattice after removing Fe_3O_4.

XPS suggests V^{4+} but not ideal for bulk oxidation states and later showed V^{4+} and V^{3+} indistinguishable.

Unit cell volume decrease with $(VO)^{2+}$ substitution may be related to Fe vacancies and Fe^{3+} formation but that is a little strange.

Another concern is size of $(VO)^{2+}$ and electrostatic repulsion between O in $(VO)^{2+}$ and O in the octahedral site of $LiFePO_4$.

Harrison and Manthiram, 2011. *Inorganic chemistry*, *50*(8), pp.3613-3620.

Is $(VO)^{2+}$ substituted for Fe^{2+} or is V^{x+} doped into $LiFePO_4$, potentially leading to distorted VO_6?

Synthesized "$LiFe_{1-x}(VO)_xPO_4$" with $0 \leq x \leq 0.25$ by a microwave-solvothermal process (<300 °C).

XRD suggests systematic substitution into crystal lattice, FTIR/electrochemistry consistent with $(VO)^{2+}$.

Fe_3O_4 impurity forms and ICP suggests iron vacancies in lattice after removing Fe_3O_4.

XPS suggests V^{4+} but not ideal for bulk oxidation states and later showed V^{4+} and V^{3+} indistinguishable.

Unit cell volume decrease with $(VO)^{2+}$ substitution may be related to Fe vacancies and Fe^{3+} formation but that is a little strange.

Another concern is size of $(VO)^{2+}$ and electrostatic repulsion between O in $(VO)^{2+}$ and O in the octahedral site of $LiFePO_4$.

The "V=O" bond in $LiVOPO_4$ indicates a distortion in the VO_6 octahedral site with long and short V-O bonds.

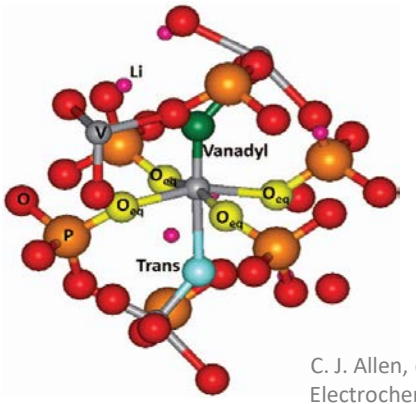

C. J. Allen, et al., J. Electrochem. Soc., 158 (12) A1250 (2011).

"$LiFe_{1-x}(VO)_xPO_4$"? "$LiFe_{1-2x}V_x\square_xPO_4$" ($V^{4+}$)? "$LiFe_{1-3x/2}V_x\square_{x/2}PO_4$" ($V^{3+}$)?

Harrison and Manthiram, 2011. *Inorganic chemistry*, *50*(8), pp.3613-3620.

V edge XANES shows oxidation state ~$V^{3.2+}$ (EELS also shows oxidation state closer to V^{3+} than V^{4+})

Synthesized according to "$LiFe_{1-x}(VO)_xPO_4$", "$LiFe_{1-2x}V_x\square_xPO_4$" ($V^{4+}$), "$LiFe_{1-3x/2}V_x\square_{x/2}PO_4$" ($V^{3+}$).

XANES measurements taken by C.U. Segre and J. Katsoudas at Argonne National Lab

XANES = X-ray absorption near edge spectroscopy

Harrison, Bridges, Paranthaman, Segre, Katsoudas, Maroni, Idrobo, Goodenough, and Manthiram, 2013. *Chemistry of Materials*, 25(5), pp.768-781.

V edge XANES shows oxidation state ~$V^{3.2+}$ (EELS also shows oxidation state closer to V^{3+} than V^{4+})

Synthesized according to "$LiFe_{1-x}(VO)_xPO_4$", "$LiFe_{1-2x}V_x\square_xPO_4$" ($V^{4+}$), "$LiFe_{1-3x/2}V_x\square_{x/2}PO_4$" ($V^{3+}$).

XANES fitting suggests **~V^{3+}** → implies ~$LiFe_{1-3x/2}V_x\square_{x/2}PO_4$.

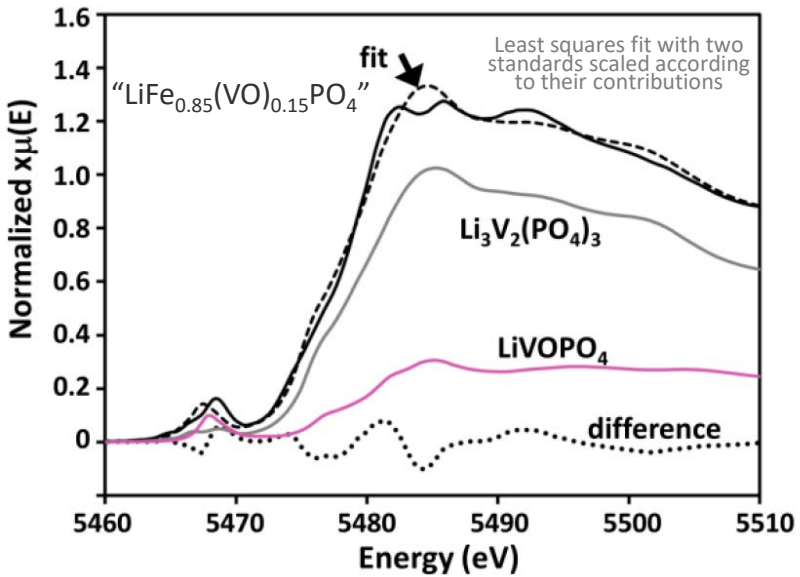

XANES = X-ray adsorption near edge spectroscopy

EELS = electron energy loss spectroscopy

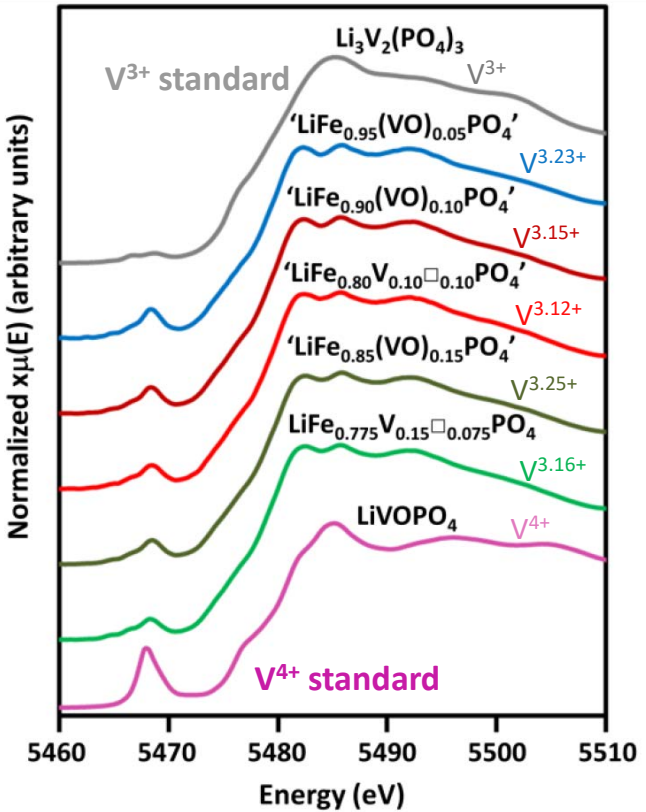

XANES measurements taken by C.U. Segre and J. Katsoudas at Argonne National Lab

XANES = X-ray absorption near edge spectroscopy

Harrison, Bridges, Paranthaman, Segre, Katsoudas, Maroni, Idrobo, Goodenough, and Manthiram, 2013. *Chemistry of Materials*, 25(5), pp.768-781.

X-ray and neutron diffraction Rietveld refinement including site occupancy analysis is consistent with $V^{3.2+}$ doping

ND measurements and ND refinement done by C. A. Bridges and M. P. Paranthaman at ORNL

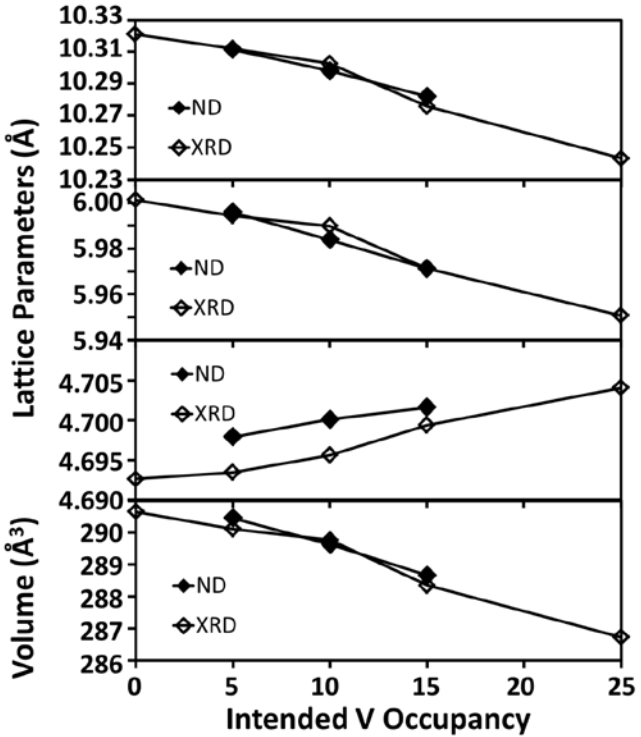

- Refinement confirms systematic volume changes.
- Refinement agrees with ICP and $LiFe_{1-3x/2}V_x\square_{x/2}PO_4$.
- 20% aliovalent doping is a huge amount!

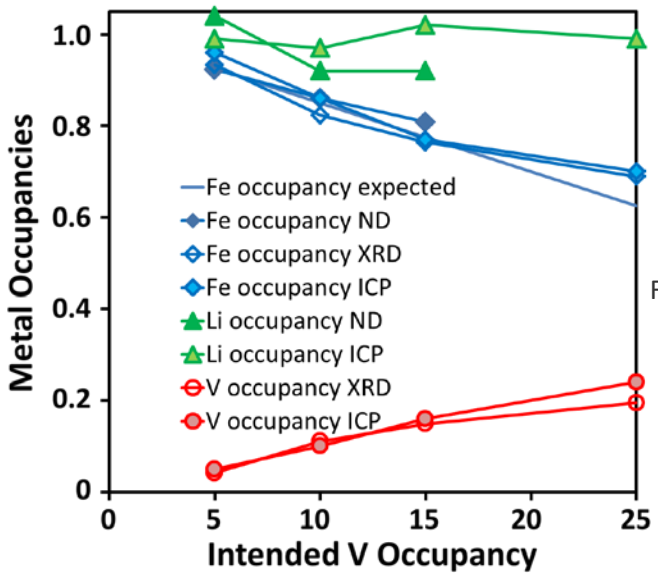

Fe expected line based on $LiFe_{1-3x/2}V_x\square_{x/2}PO_4$

Harrison, Bridges, Paranthaman, Segre, Katsoudas, Maroni, Idrobo, Goodenough, and Manthiram, 2013. *Chemistry of Materials*, 25(5), pp.768-781.

Characterizing pristine and heated samples can help us understand doping levels

Sample	Furnace Temp.	Furnace Time	Furnace Atmosphere
MW-LFP-unheated	N/A	N/A	N/A
MW-LFVP-unheated	N/A	N/A	N/A
MW-LFVP-H_2-500-6h	500 °C	6 h	5 % H_2 – 95 % Ar
MW-LFVP-H_2-600-6h	600 °C	6 h	5 % H_2 – 95 % Ar
MW-LFVP-H_2-700-6h	700 °C	6 h	5 % H_2 – 95 % Ar
MW-LFVP-Ar-500-6h	500 °C	6 h	Ar
MW-LFVP-Ar-600-6h	600 °C	6 h	Ar
MW-LFVP-Ar-700-6h	700 °C	6 h	Ar
MW-LFVP-Ar-500-15h	500 °C	15 h	Ar
MW-LFVP-Ar-600-15h	600 °C	15 h	Ar
MW-LFVP-Ar-700-15h	700 °C	15 h	Ar
MW-LFVP-air-500-4h	500 °C	4 h	air
MW-LFVP-air-700-4h	700 °C	4 h	air

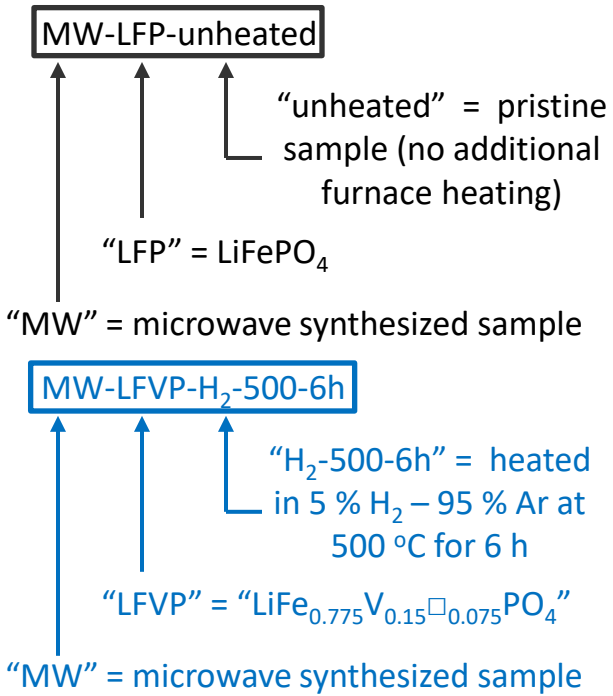

Harrison, Bridges, Paranthaman, Segre, Katsoudas, Maroni, Idrobo, Goodenough, and Manthiram, 2013. *Chemistry of Materials*, 25(5), pp.768-781.

Conventional "$LiFe_{0.775}V_{0.15}\square_{0.075}PO_4$" and $Li_3V_2(PO_4)_3$ synthesized by ball milling and heating to compare to heated MW-ST samples

Sample	Intended Product	Furnace Temp.	Furnace Time	Furnace Atmosphere
CONV-LFP-Ar-700-6h	$LiFePO_4$	700 °C	6 h	Ar
CONV-LFVP-H_2-500-6h	"$LiFe_{0.775}V_{0.15}\square_{0.075}PO_4$"	500 °C	6 h	5 % H_2 – 95 % Ar
CONV-LFVP-H_2-600-6h	"$LiFe_{0.775}V_{0.15}\square_{0.075}PO_4$"	600 °C	6 h	5 % H_2 – 95 % Ar
CONV-LFVP-H_2-700-6h	"$LiFe_{0.775}V_{0.15}\square_{0.075}PO_4$"	700 °C	6 h	5 % H_2 – 95 % Ar
CONV-LFVP-Ar-500-6h	"$LiFe_{0.775}V_{0.15}\square_{0.075}PO_4$"	500 °C	6 h	Ar
CONV-LFVP-Ar-600-6h	"$LiFe_{0.775}V_{0.15}\square_{0.075}PO_4$"	600 °C	6 h	Ar
CONV-LFVP-Ar-700-6h	"$LiFe_{0.775}V_{0.15}\square_{0.075}PO_4$"	700 °C	6 h	Ar
CONV-LVP3-H_2-500-6h	$Li_3V_2(PO_4)_3$	500 °C	6 h	5 % H_2 – 95 % Ar
CONV-LVP3-H_2-600-6h	$Li_3V_2(PO_4)_3$	600 °C	6 h	5 % H_2 – 95 % Ar
CONV-LVP3-H_2-700-6h	$Li_3V_2(PO_4)_3$	700 °C	6 h	5 % H_2 – 95 % Ar
CONV-LVP3-Ar-500-6h	$Li_3V_2(PO_4)_3$	500 °C	6 h	Ar
CONV-LVP3-Ar-600-6h	$Li_3V_2(PO_4)_3$	600 °C	6 h	Ar
CONV-LVP3-Ar-700-6h	$Li_3V_2(PO_4)_3$	700 °C	6 h	Ar

CONV-LFVP-H_2-500-6h

"LFVP" = "$LiFe_{0.775}V_{0.15}\square_{0.075}PO_4$"

"CONV" = conventionally made sample – no MW heating

CONV-LVP3-H_2-500-6h

"LVP3" = $Li_3V_2(PO_4)_3$

"CONV" = conventionally made sample – no MW heating

Harrison, Bridges, Paranthaman, Segre, Katsoudas, Maroni, Idrobo, Goodenough, and Manthiram, 2013. *Chemistry of Materials*, 25(5), pp.768-781.

XRD Rietveld refinement shows 15% V doping only stable through MW-ST

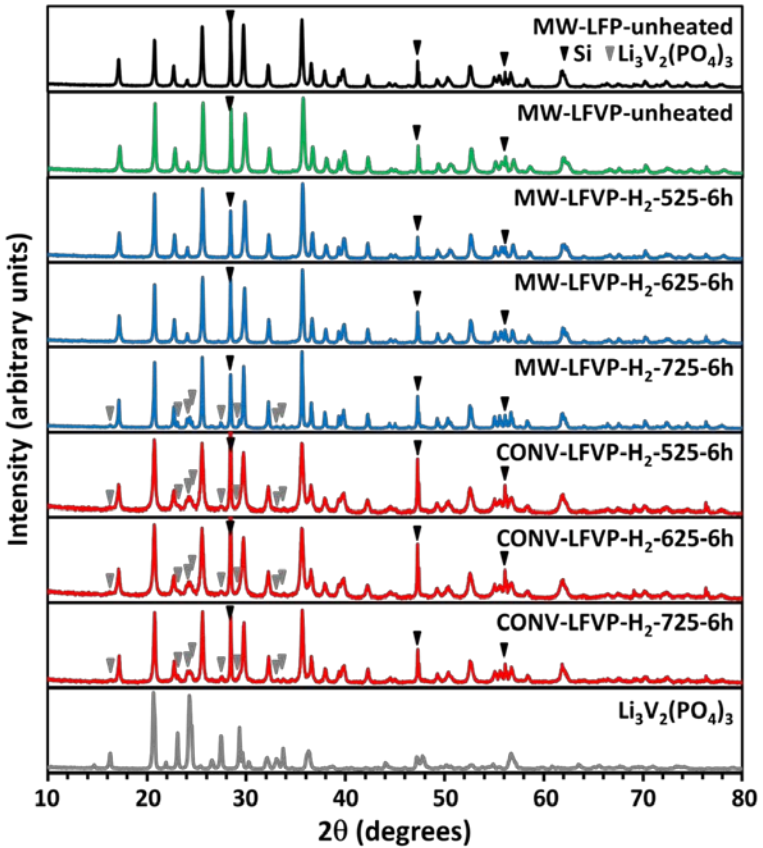

Heating MW-ST → $Li_3V_2(PO_4)_3$ at 725 °C.

All conventional samples → $Li_3V_2(PO_4)_3$.

"LFVP" = "$LiFe_{0.775}V_{0.15}\square_{0.075}PO_4$"

Harrison, Bridges, Paranthaman, Segre, Katsoudas, Maroni, Idrobo, Goodenough, and Manthiram, 2013. *Chemistry of Materials*, 25(5), pp.768-781.

XRD Rietveld refinement shows 15% V doping only stable through MW-ST

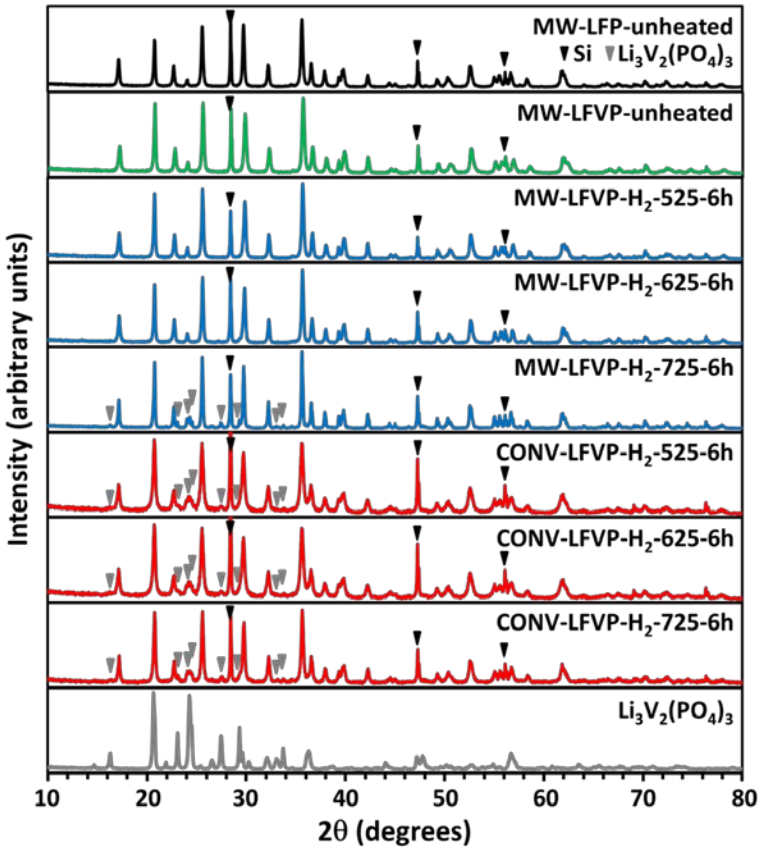

- Heating MW-ST → $Li_3V_2(PO_4)_3$ at 725 °C.
- All conventional samples → $Li_3V_2(PO_4)_3$.
- V doping at low temperature is metastable.

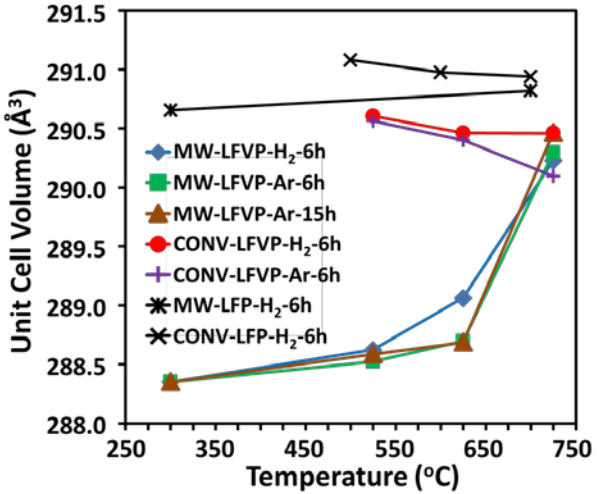

"LFVP" = "$LiFe_{0.775}V_{0.15}\square_{0.075}PO_4$"

Harrison, Bridges, Paranthaman, Segre, Katsoudas, Maroni, Idrobo, Goodenough, and Manthiram, 2013. *Chemistry of Materials*, 25(5), pp.768-781.

Maximum aliovalent V doping content is a temperature dependent

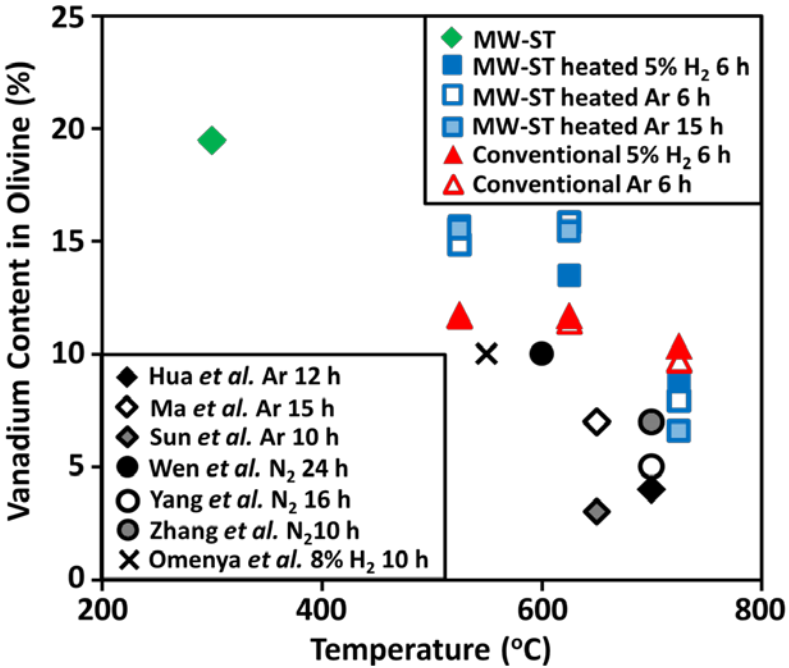

Rietveld refinement: V occupancy decreases with increasing temperature.

Conventional synthesis: only ~10-11 % V doping possible.

Harrison, Bridges, Paranthaman, Segre, Katsoudas, Maroni, Idrobo, Goodenough, and Manthiram, 2013. *Chemistry of Materials*, 25(5), pp.768-781.

Cyclic voltammetry shows V activity

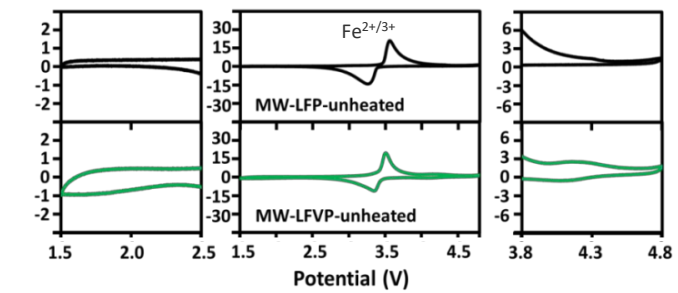

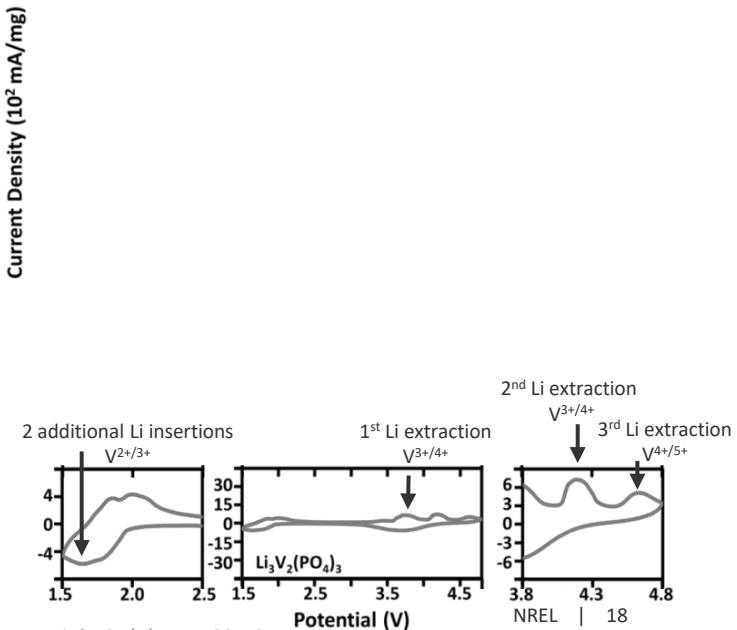

Harrison, Bridges, Paranthaman, Segre, Katsoudas, Maroni, Idrobo, Goodenough, and Manthiram, 2013. *Chemistry of Materials*, 25(5), pp.768-781.

Cyclic voltammetry shows V activity

- V activity peaks shift and sharpen with heating.
- Only slight changes after heating MW-ST 525-625 °C.
- $Li_3V_2(PO_4)_3$ in MW-ST sample heated at 725 °C.

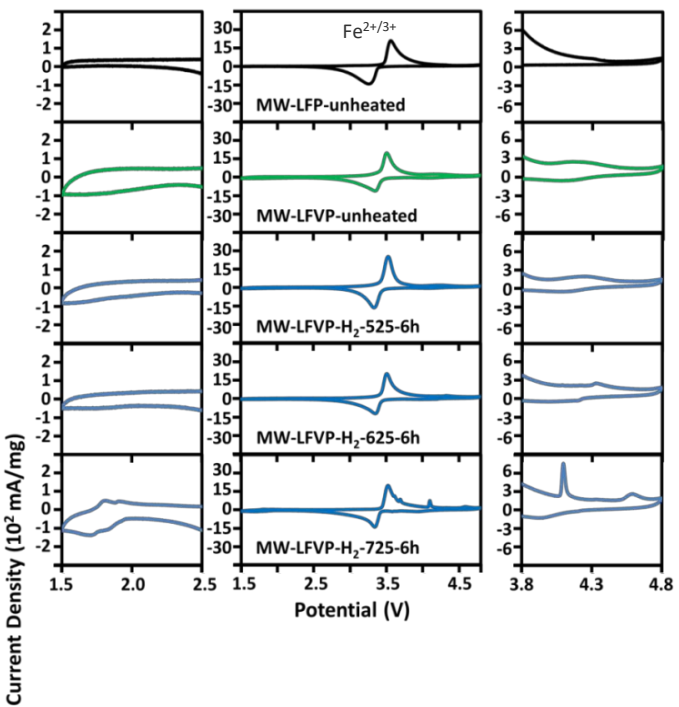

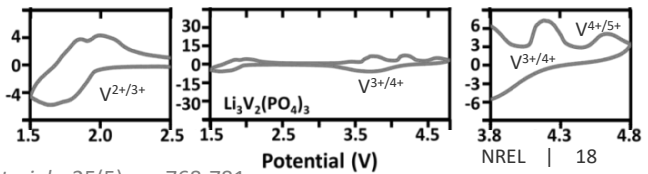

Harrison, Bridges, Paranthaman, Segre, Katsoudas, Maroni, Idrobo, Goodenough, and Manthiram, 2013. *Chemistry of Materials*, 25(5), pp.768-781.

Cyclic voltammetry shows V activity

- V activity peaks shift and sharpen with heating.
- Only slight changes after heating MW-ST 525-625 °C.
- $Li_3V_2(PO_4)_3$ in MW-ST sample heated at 725 °C.
- $Li_3V_2(PO_4)_3$ in all conventionally made samples.

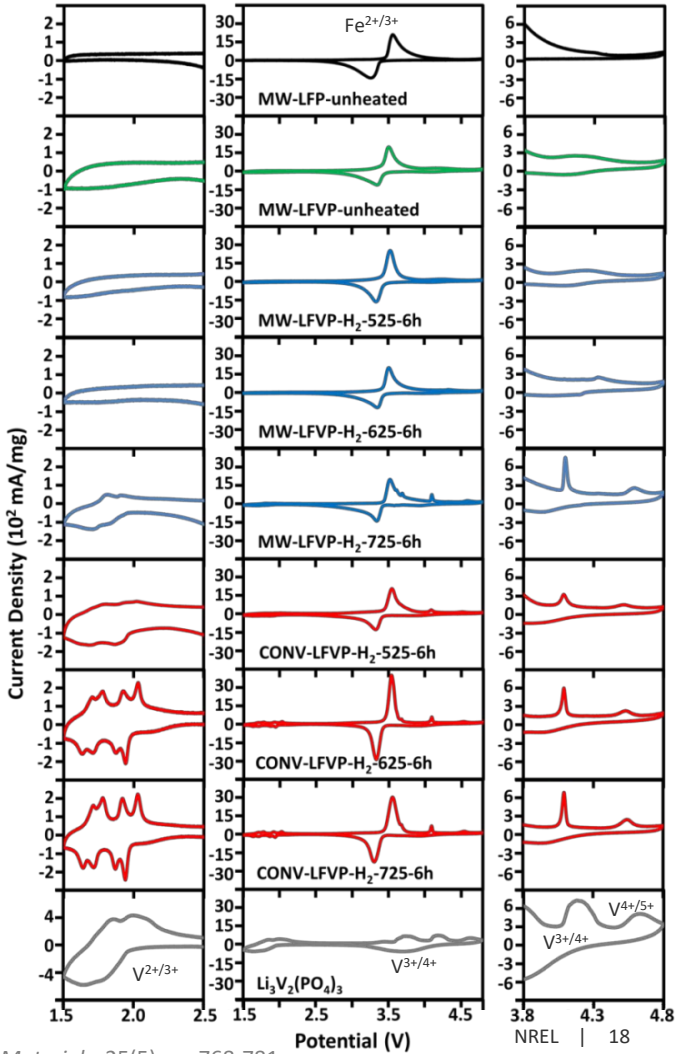

Harrison, Bridges, Paranthaman, Segre, Katsoudas, Maroni, Idrobo, Goodenough, and Manthiram, 2013. *Chemistry of Materials*, 25(5), pp.768-781.

Galvanostatic cycling data shows better cycle stability in doped samples but lower capacity due to Fe site vacancies

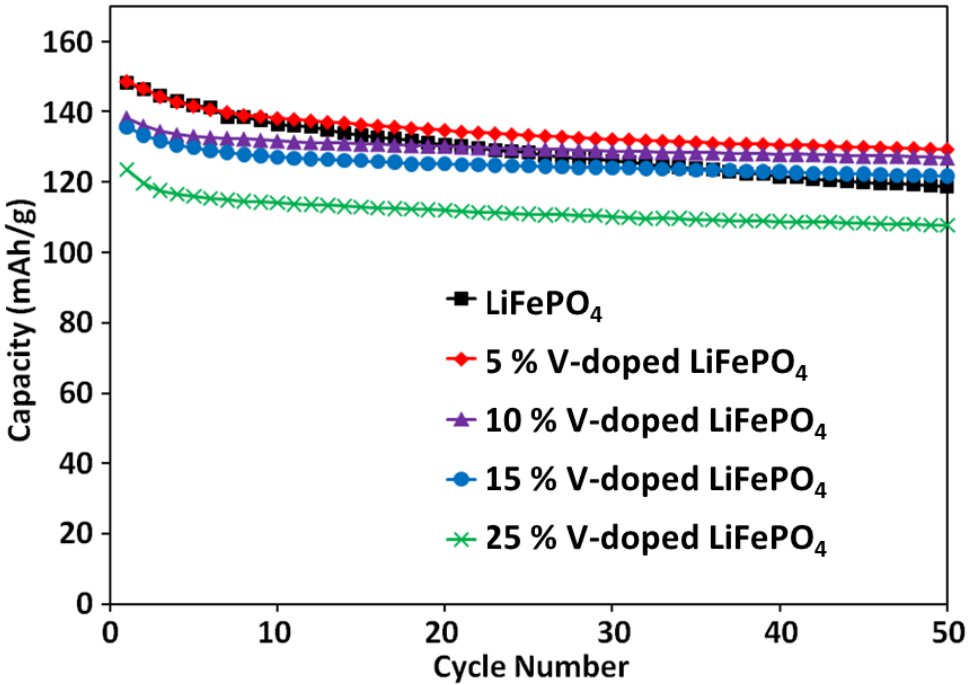

Harrison, Bridges, Paranthaman, Segre, Katsoudas, Maroni, Idrobo, Goodenough, and Manthiram, 2013. *Chemistry of Materials*, 25(5), pp.768-781.

Conclusions

X-ray/neutron refinement, ICP, EELS, and XANES confirm $LiFe_{1-3x/2}V_x\square_{x/2}PO_4$ rather than $LiFe_{1-x}(VO)_xPO_4$ with ~V^{3+} + Fe site vacancies that substitute for Fe^{2+}.

$LiFe_{1-3x/2}V_x\square_{x/2}PO_4$ with x = 0.2 can be synthesized by MW-ST, but heating leads to decreasing dopant levels and $Li_3V_2(PO_4)_3$ impurities with increased temperature.

Conventional high temperature solid state $LiFe_{1-3x/2}V_x\square_{x/2}PO_4$ synthesis results in dopant levels limited to ~10% and forms $Li_3V_2(PO_4)_3$ impurities at all temperatures.

Low temperature MW-ST provides access to metastable phase and higher doping.

X-ray techniques provide remarkable insight for understanding battery materials!

Harrison, Bridges, Paranthaman, Segre, Katsoudas, Maroni, Idrobo, Goodenough, and Manthiram, 2013. *Chemistry of Materials*, 25(5), pp.768-781.

Outline

Introduction to rechargeable Li batteries

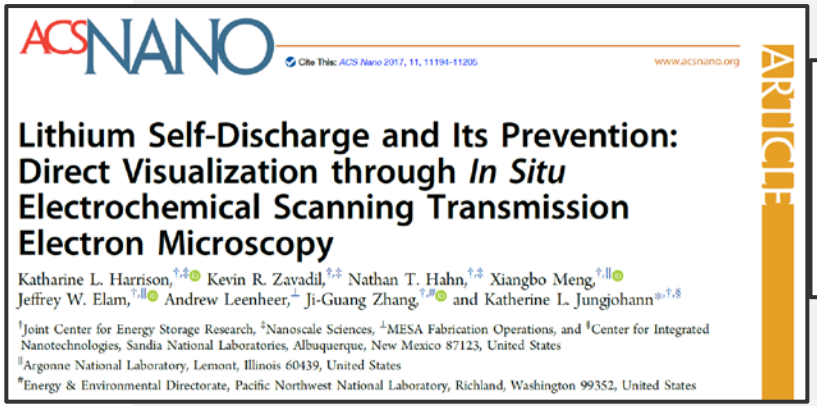

ACS NANO

Cite This: ACS Nano 2017, 11, 11194−11205 www.acsnano.org

ARTICLE

Lithium Self-Discharge and Its Prevention: Direct Visualization through *In Situ* Electrochemical Scanning Transmission Electron Microscopy

Katharine L. Harrison,[†,‡] Kevin R. Zavadil,[†,‡] Nathan T. Hahn,[†,‡] Xiangbo Meng,[†,∥] Jeffrey W. Elam,[†,∥] Andrew Leenheer,[⊥] Ji-Guang Zhang,[†,#] and Katherine L. Jungjohann[*,†,§]

[†]Joint Center for Energy Storage Research, [‡]Nanoscale Sciences, [⊥]MESA Fabrication Operations, and [§]Center for Integrated Nanotechnologies, Sandia National Laboratories, Albuquerque, New Mexico 87123, United States

[∥]Argonne National Laboratory, Lemont, Illinois 60439, United States

[#]Energy & Environmental Directorate, Pacific Northwest National Laboratory, Richland, Washington 99352, United States

89 Powder Diffraction **35** (2), June 2020 0885-7156/2020/35(2)/89/9/$18.00

PROCEEDINGS PAPER

Use of a Be-dome holder for texture and strain characterization of Li metal thin films via $\sin^2(\psi)$ methodology

Mark A. Rodriguez [a)] Katharine L. Harrison, Subrahmanyam Goriparti, James J. M. Griego, Brad L. Boyce, and Brian R. Perdue

Sandia National Laboratories, Albuquerque, New Mexico 87185-1411, USA

Example 2: understanding stress in Li metal anodes using X-ray techniques

Background

Li metal anodes could enable lighter and smaller batteries.

Li electrodeposition forms high aspect ratio morphologies that cause short circuits, consume Li/electrolyte, and cycle poorly.

Applying pressure during cycling can improve Coulombic efficiency (CE), morphology, and safety.

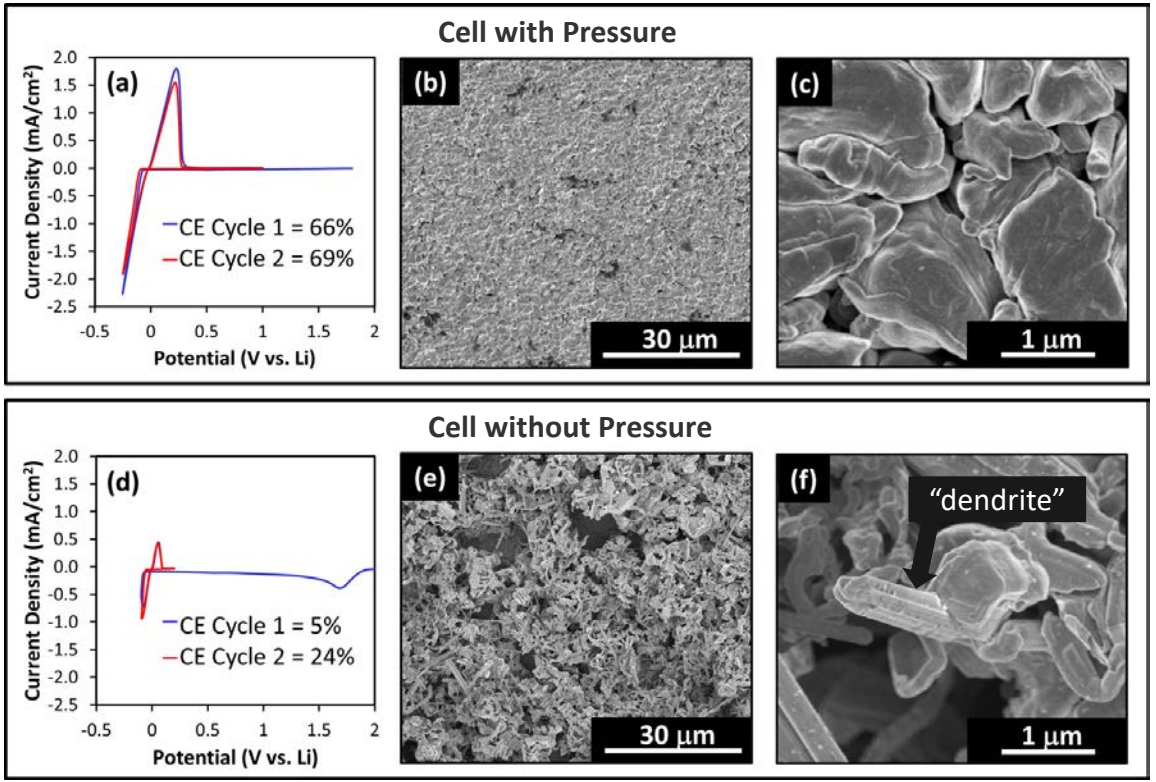

Harrison, Zavadil, Hahn, Meng, Elam, Leenheer, Zhang, and Jungjohann, 2017. ACS nano, 11(11), pp.11194-11205.

Motivation

Our Li metal cycling studies show that mild applied pressure can improve Li cycling but too much pressure can exacerbate short circuits.

Harrison, et al., 2021. *ACS Applied Materials & Interfaces*, *13*(27), pp.31668-31679.
Harrison, Merrill, Long, Randolph, Goriparti, Christian, Warren, Roberts, Harris, Perry, and Jungjohann, 2021. *Iscience*, *24*(12).
Jungjohann, Gannon, Goriparti, Randolph, Merrill, Johnson, Zavadil, Harris, and Harrison, 2021. *ACS Energy Letters*, *6*(6), pp.2138-2144.

Li is a soft metal, so how can it pierce the separator and cause short circuits?

Before this study, literature had suggested Li metal can be work hardened.

Hypothesis: applied pressure causes work hardening in Li metal, which could make it easier to pierce the separator and cause short circuits.

Can we measure evidence of Li work hardening (residual strain) with XRD?

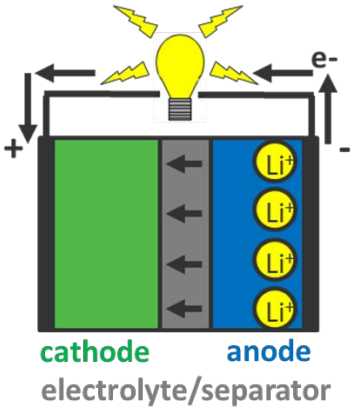

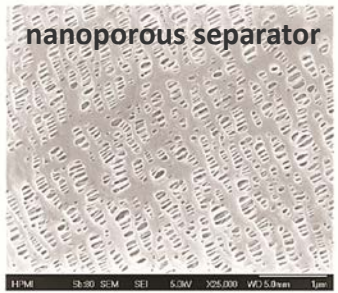

Rajagopalan Kannan, D.R., Terala, P.K., Moss, P.L. and Weatherspoon, M.H., 2018. *International Journal of Electrochemistry*, *2018*(1), p.1925708.

Rodriguez, Harrison, Goriparti, Griego, Boyce, and Perdue, 2020. Powder Diffraction, 35(2), pp.89-97.

Electrochemical method

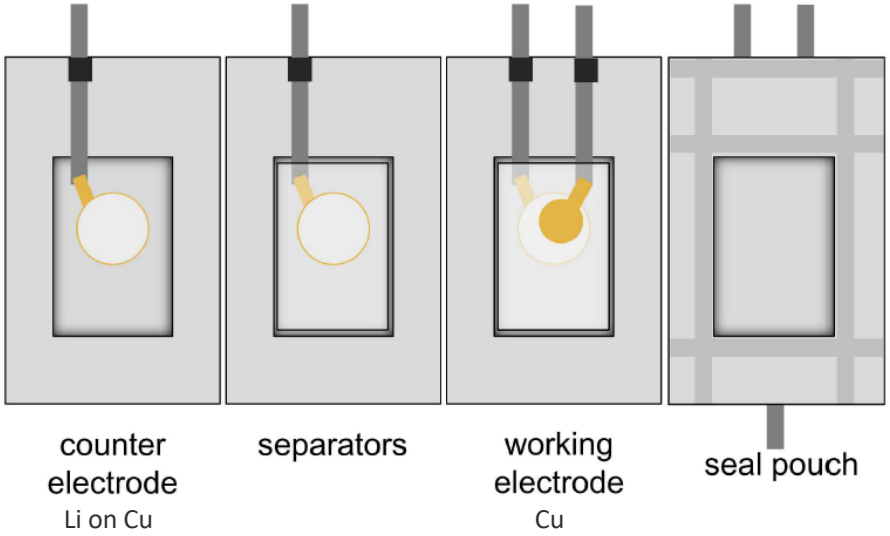

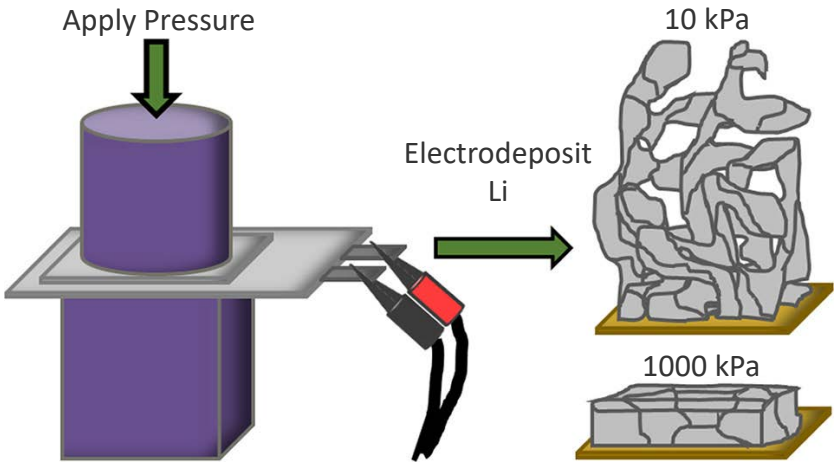

4 mA/cm^2 to 40 mAh/cm^2 (195 µm equivalent Li thickness if assume fully dense)

- Fabricate pouch cells and electrodeposit Li on Cu working electrode.
- Disassemble pouch cell and extract working electrode.
- Sin$^2\psi$ XRD method to understand residual strain in Li.

Harrison, et al., 2021. *ACS Applied Materials & Interfaces*, *13*(27), pp.31668-31679.
Rodriguez, Harrison, Goriparti, Griego, Boyce, and Perdue, 2020. Powder Diffraction, 35(2), pp.89-97.

$Sin^2\psi$ analysis using tilt-a-whirl data processing and analysis

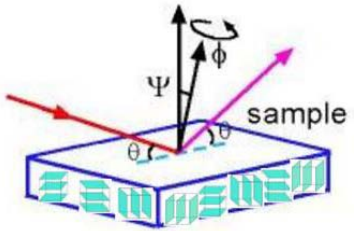

http://mrlweb.mrl.ucsb.edu/centralfacilities/x-ray/basics
Rodriguez, Denver X-ray conference workshop, 2013.

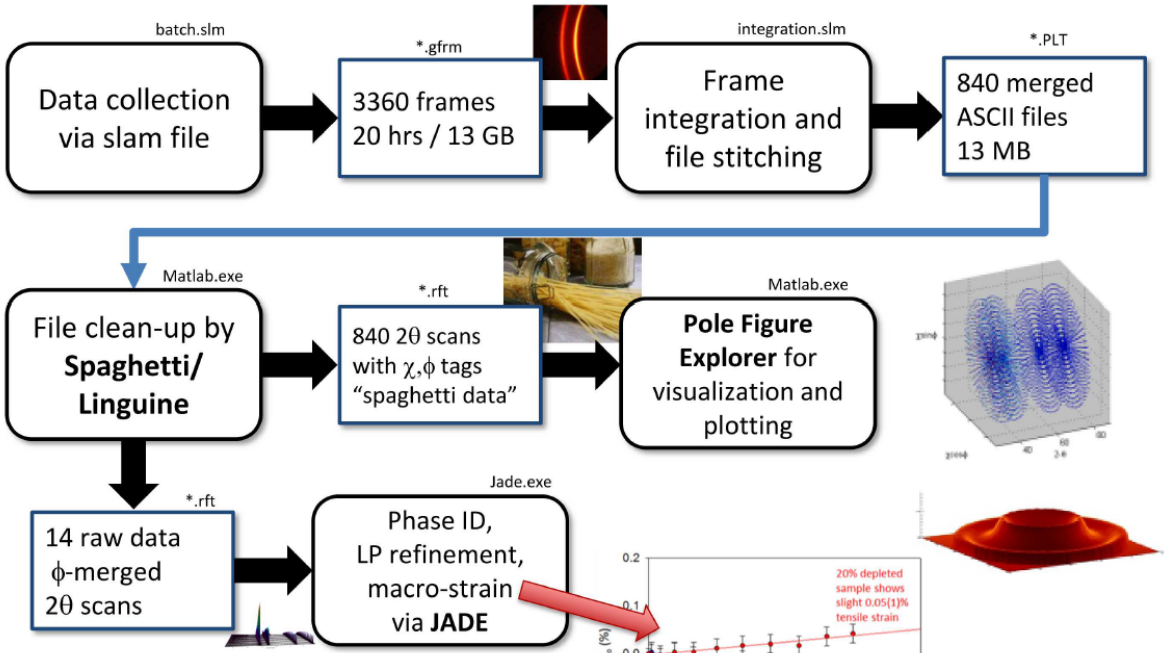

TILT-A-WHIRL is a texture analysis package for 3D rendering of pole figures using Matlab.

Rodriguez, Pearl, Van Benthem, Griego, Pillars, 2013. Powder Diffraction, 28(2), pp.81-89.

Li samples loaded in Be dome holder in Ar-filled glove box and then holder is mounted on texture cradle

Rodriguez, Boyle, Yang, and Harris, 2008.
Powder Diffraction, 23(2), pp.121-124.

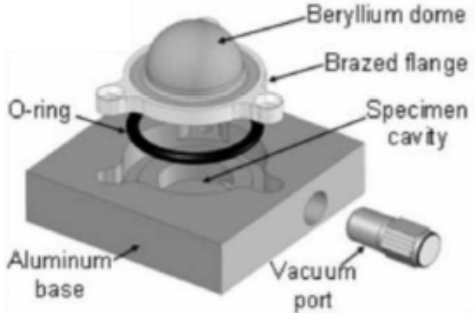

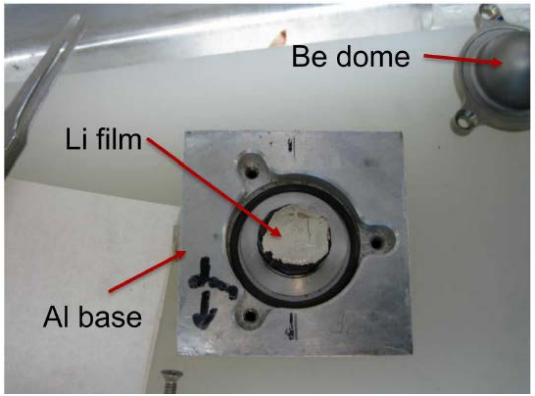

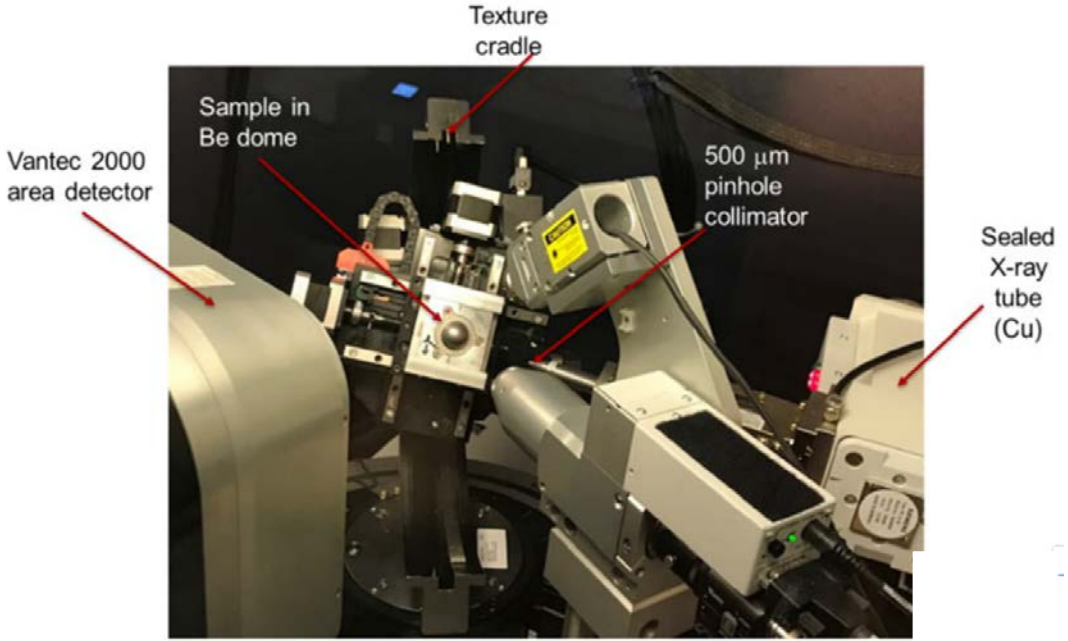

Rodriguez, Harrison, Goriparti, Griego, Boyce, and Perdue, 2020. Powder Diffraction, 35(2), pp.89-97.

Li (211) does not overlap with anything and can be used for macrostrain analysis

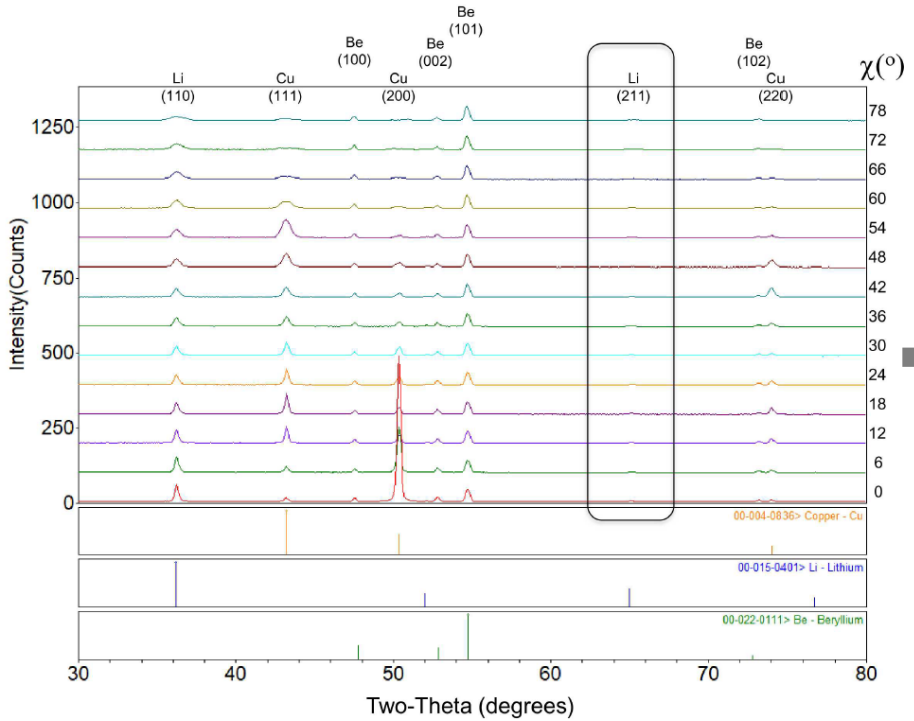

Li electrodeposited at 1000 kPa

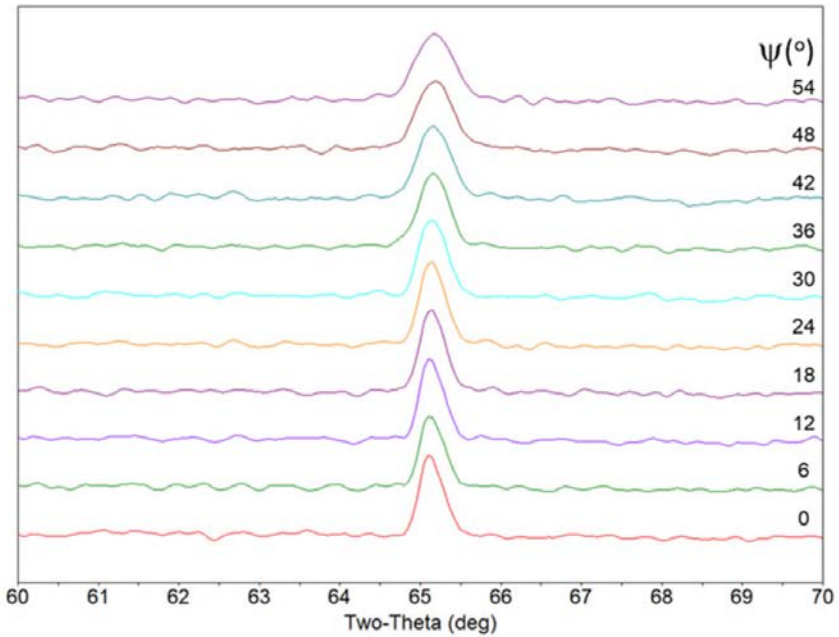

60 ϕ-merged scans for each Ψ tilt

Rodriguez, Harrison, Goriparti, Griego, Boyce, and Perdue, 2020. Powder Diffraction, 35(2), pp.89-97.

Li electrodeposited at 1000 kPa (but not at 10 kPa) exhibit residual strain, which is evidence of work hardening

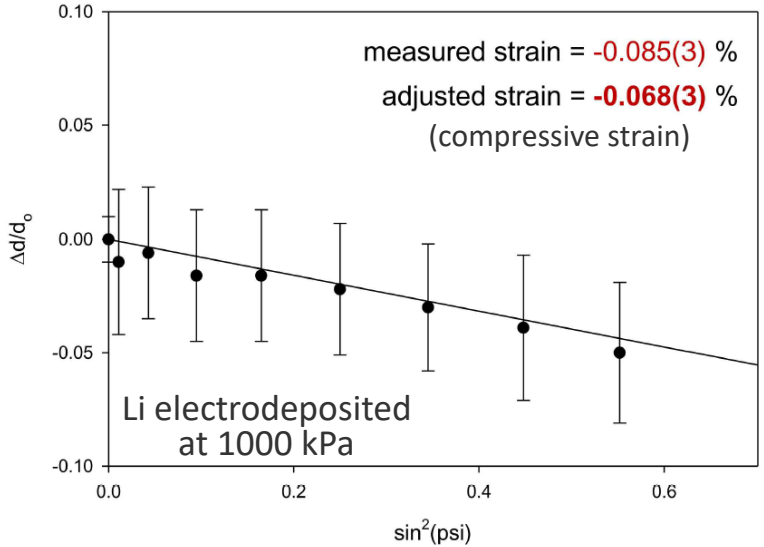

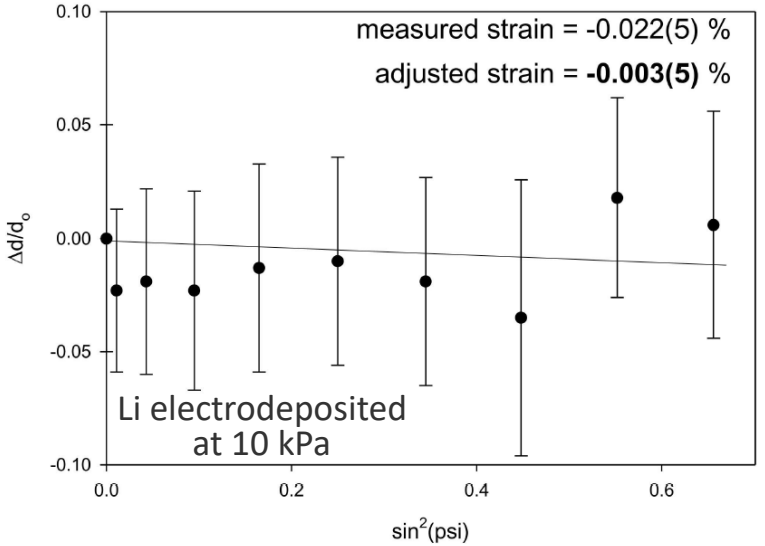

Roughly estimate residual stress using untextured Young's modulus for Li of ~ 5 GPa = 3.4 MPa.

3.4 MPa is a substantial fraction of yield strength of Li (16 MPa, though literature ranges <1-100 MPa).

Varied yield strength in literature may be caused by processing-dependent work hardening.

Applied pressure during Li electrodeposition causes work hardening. Can that make stronger dendrites?

Rodriguez, Harrison, Goriparti, Griego, Boyce, and Perdue, 2020. Powder Diffraction, 35(2), pp.89-97.

Conclusions

Developed method to detect residual strain in electrodeposited Li metal using tilt-a-whirl XRD.

Detected residual in-plane strain in Li electrodeposited under 1000 kPa pressure but not under 10 kPa.

Residual strain suggests work hardening occurs during high pressure electrodeposition and that may impact how dendrites form and their ability to cause short circuits.

This is consistent with our data showing that high pressure can lead to increased short circuits.

X-ray techniques provide remarkable insight for understanding battery materials!

Rodriguez, Harrison, Goriparti, Griego, Boyce, and Perdue, 2020. Powder Diffraction, 35(2), pp.89-97.

I presented some relatively old studies but using X-ray techniques in all current projects too…

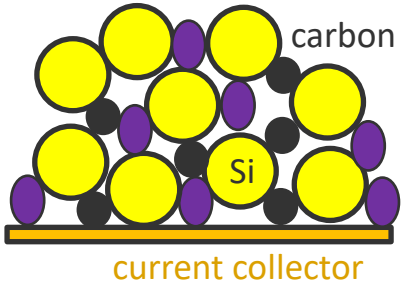

Work on large Si anode consortium for batteries and the morphology/architecture of the electrodes is very important to understand their performance.

Donal Finegan will discuss!

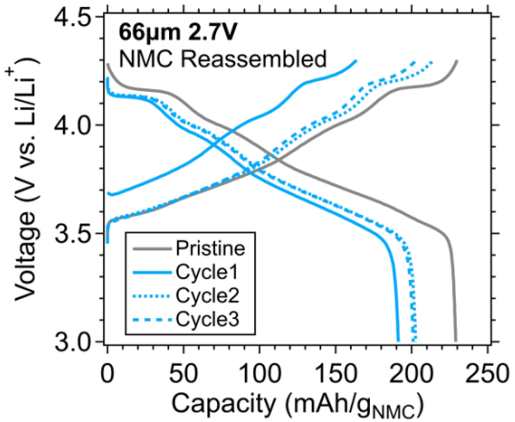

Work on designing batteries for microgrid stationary storage to charge electric vehicles, where long cycle life and understanding degradation is critical.

Noah Schorr will discuss!

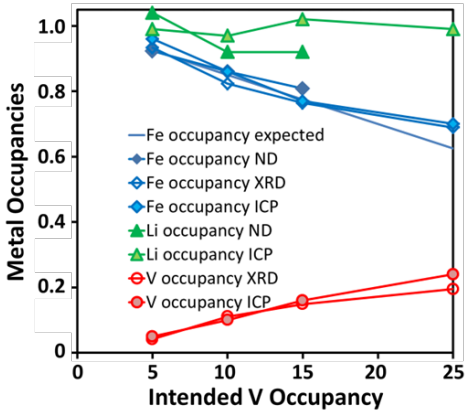

Work on understanding how impurities in domestically sourced precursors for $LiFePO_4$ batteries change performance and how impurities dope the structure.

In progress, but full circle…

Work performed while at:

University of Texas at Austin
- National Science Foundation
- DOE, Basic Energy Sciences
- DOE, Vehicle Technologies Office

Sandia National Labs
- Lab Directed Research and Development

Thank you

www.nrel.gov

Katie.Harrison@nrel.gov

NREL/PR-5K00-90753

This work was authored in part by the National Renewable Energy Laboratory, operated by Alliance for Sustainable Energy, LLC, for the U.S. Department of Energy (DOE) under Contract No. DE-AC36-08GO28308. Funding was provided by the U.S. Department of Energy's Vehicle Technologies Office under the Behind-the-Meter Storage (BTMS) Consortium directed by Fernando Salcedo and managed by Anthony Burrell. Funding provided by U.S. Department of Energy Office of Energy Efficiency and Renewable Energy Solar Energy Technologies Office. The views expressed in the article do not necessarily represent the views of the DOE or the U.S. Government. The U.S. Government retains and the publisher, by accepting the article for publication, acknowledges that the U.S. Government retains a nonexclusive, paid-up, irrevocable, worldwide license to publish or reproduce the published form of this work, or allow others to do so, for U.S. Government purposes. This work was authored in part by Sandia National Laboratories. Sandia National Laboratories is a multimission laboratory managed and operated by National Technology & Engineering Solutions of Sandia, LLC, a wholly owned subsidiary of Honeywell International Inc., for the U.S. Department of Energy's National Nuclear Security Administration under contract DE-NA0003525.

Backup Slides

Galvanostatic cycling

$V^{4+/5+}$ redox active? $V^{3+/4+}$ redox active?

Increased solid solution between $FePO_4$/$LiFePO_4$.

$Fe^{2+/3+}$ coexistence without phase boundary could improve electronic conductivity by increasing charge carriers (conductivity from small polaron hopping of Fe^{3+} holes or Fe^{2+} electrons).

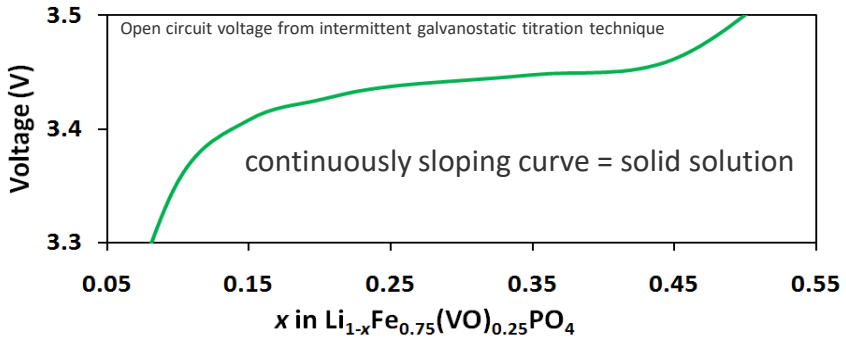

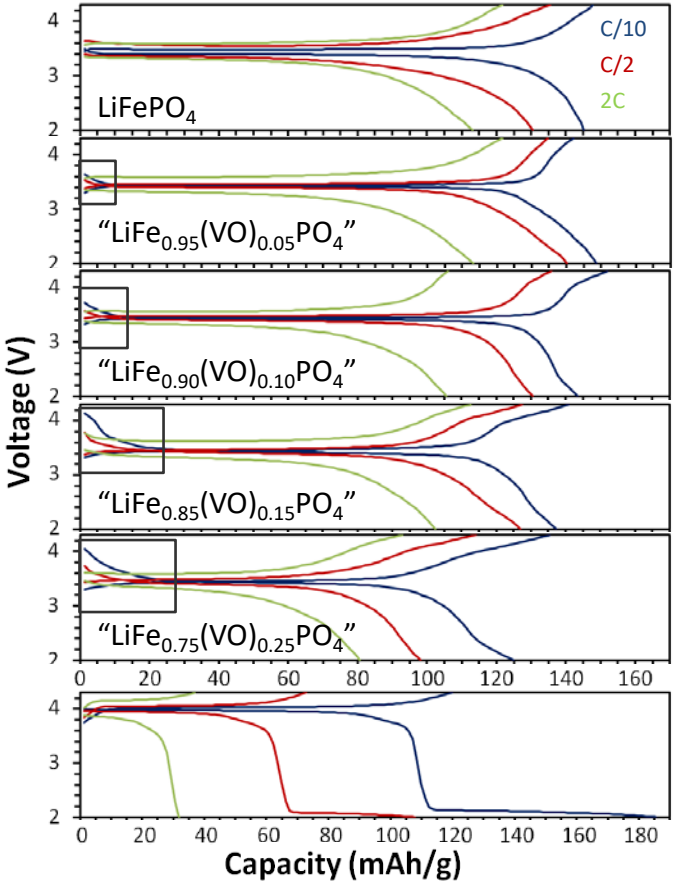

Harrison and Manthiram, 2011. *Inorganic chemistry*, *50*(8), pp.3613-3620.

Cyclic Voltammetry

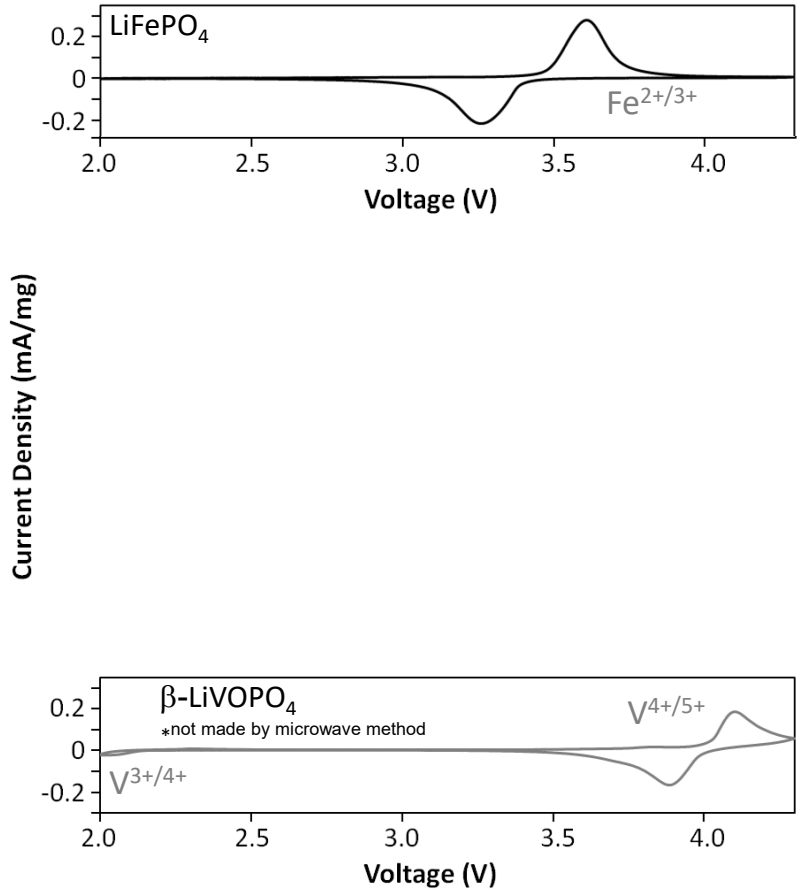

Harrison and Manthiram, 2011. *Inorganic chemistry*, *50*(8), pp.3613-3620.

Cyclic Voltammetry

Redox activity largely similar to $LiFePO_4$.

Less $Fe^{2+/3+}$ peak polarization with increased $(VO)^{2+}$ → better kinetics.

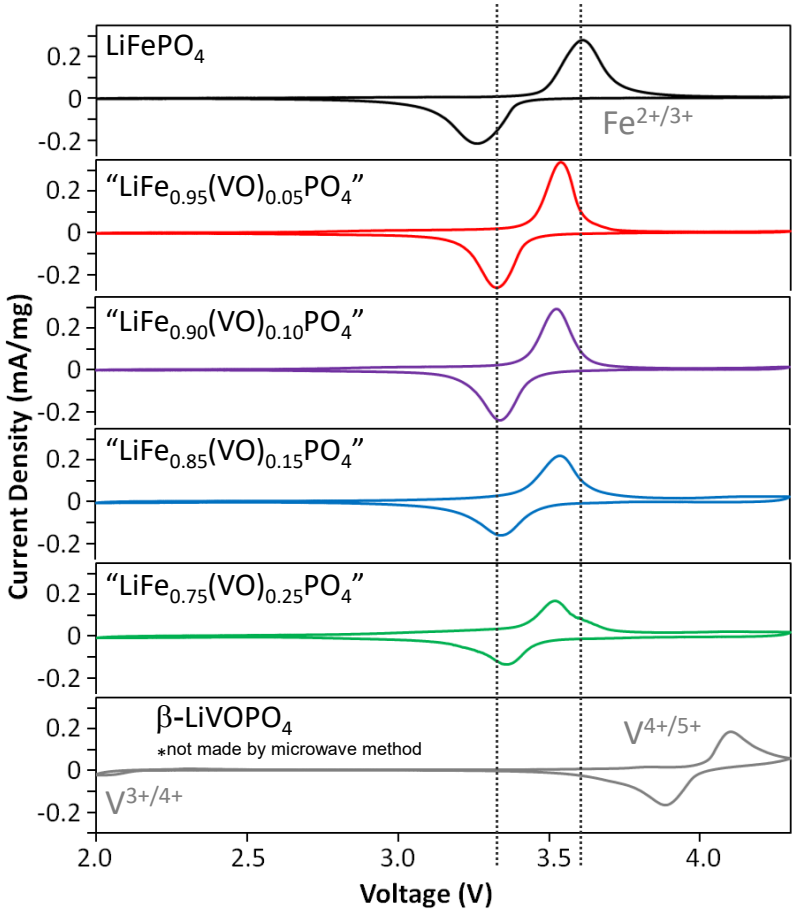

Harrison and Manthiram, 2011. *Inorganic chemistry*, *50*(8), pp.3613-3620.

STEM/EDS mapping shows no V impurity for pristine MW-ST samples, but V impurities for heated MW-ST and all conventional samples

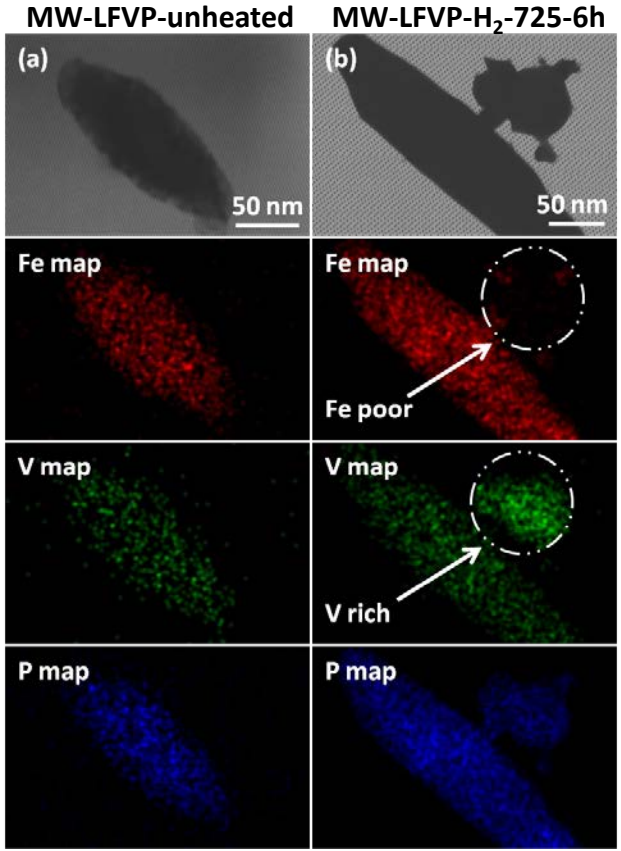

STEM = scanning transmission electron microscopy

EDS = energy dispersive X-ray spectroscopy

Harrison, Bridges, Paranthaman, Segre, Katsoudas, Maroni, Idrobo, Goodenough, and Manthiram, 2013. *Chemistry of Materials*, 25(5), pp.768-781.

STEM/EDS mapping shows no V impurity for pristine MW-ST samples, but V impurities for heated MW-ST and all conventional samples

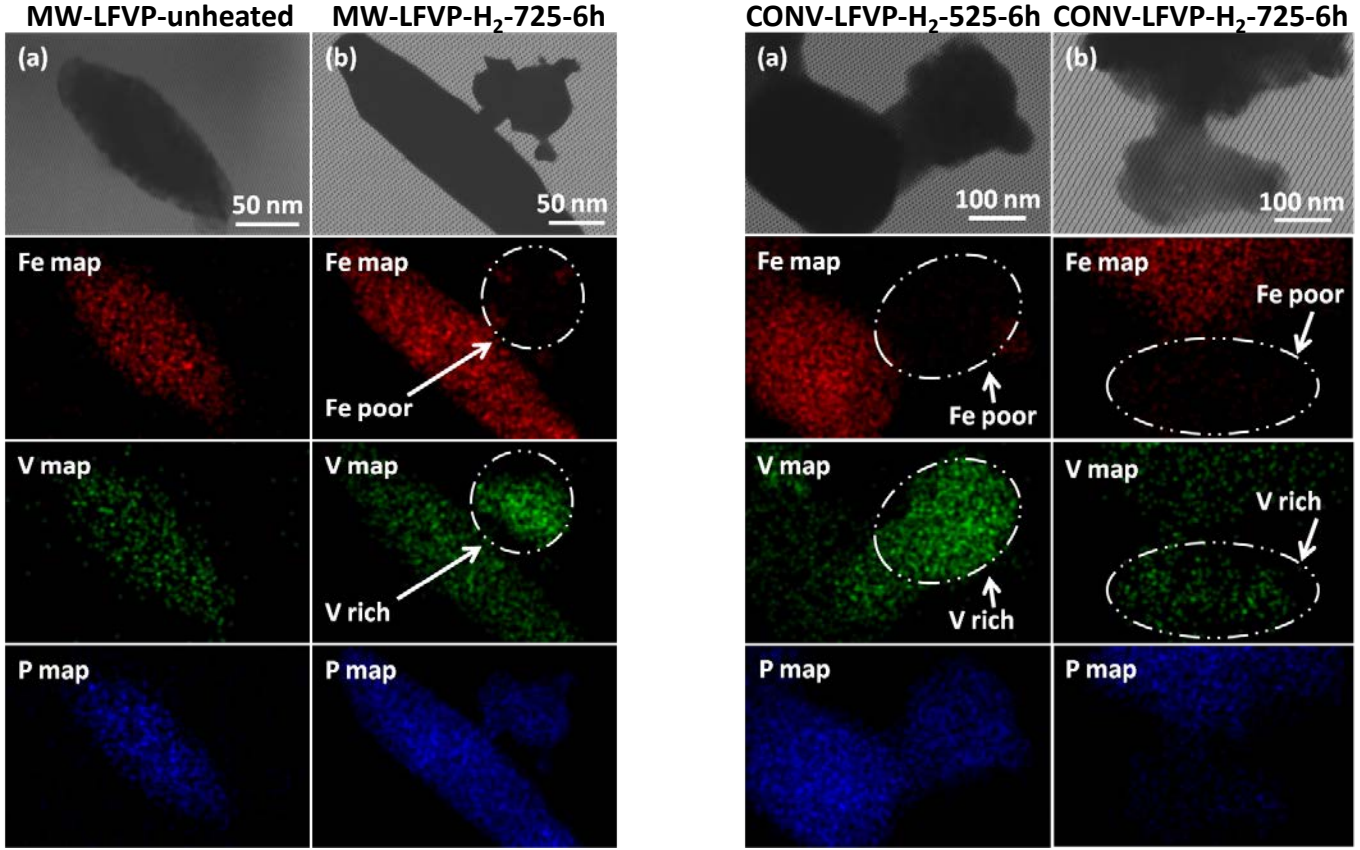

STEM = scanning transmission electron microscopy

EDS = energy dispersive X-ray spectroscopy

Harrison, Bridges, Paranthaman, Segre, Katsoudas, Maroni, Idrobo, Goodenough, and Manthiram, 2013. *Chemistry of Materials*, 25(5), pp.768-781.

Heating MW-ST samples in varied environments

The olivine phase was not stable in air and $Li_3Fe_2(PO_4)_3$ formed as expected.

$Li_3V_2(PO_4)_3$ impurity was obvious in samples heated at 700 °C in reducing atmospheres.

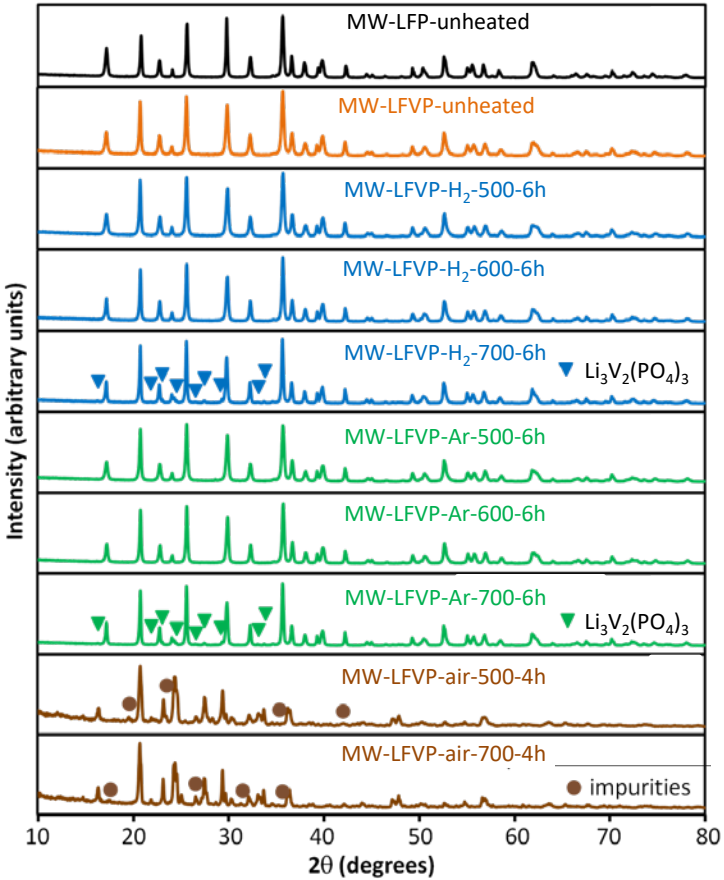

Harrison, Bridges, Paranthaman, Segre, Katsoudas, Maroni, Idrobo, Goodenough, and Manthiram, 2013. *Chemistry of Materials*, 25(5), pp.768-781.

Raman shows no evidence of a V=O bond!!!

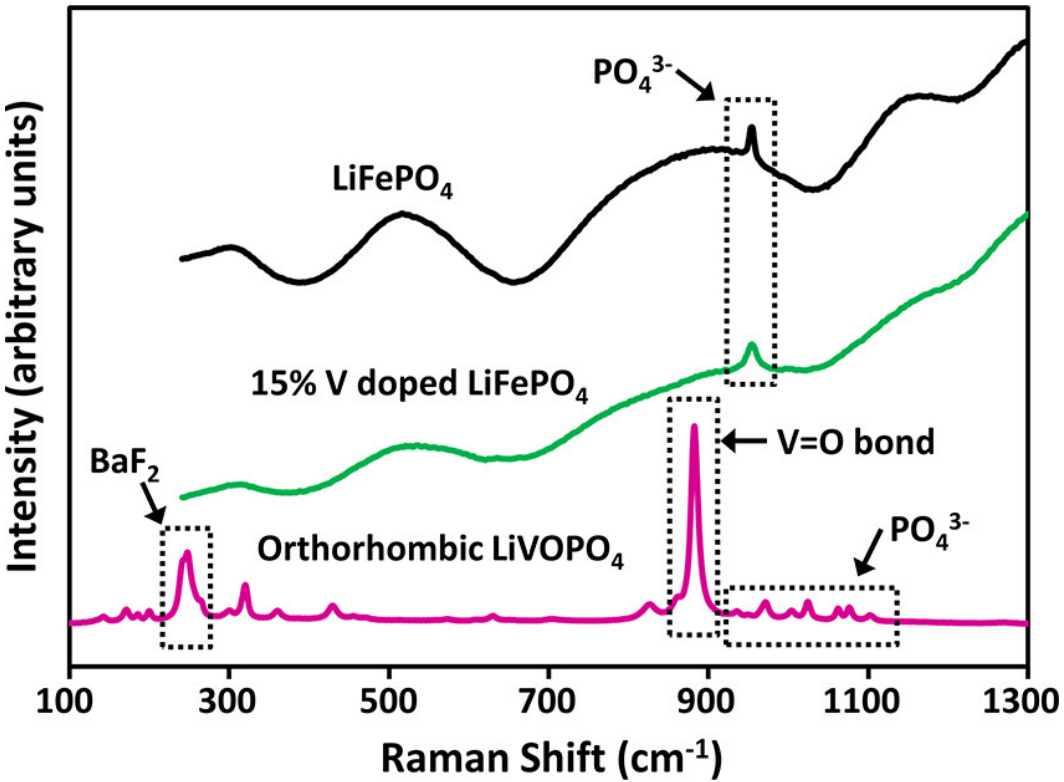

Harrison, Bridges, Paranthaman, Segre, Katsoudas, Maroni, Idrobo, Goodenough, and Manthiram, 2013. *Chemistry of Materials*, 25(5), pp.768-781.

FTIR of Heated $LiFe_{0.775}V_{0.15}\square_{0.075}PO_4$

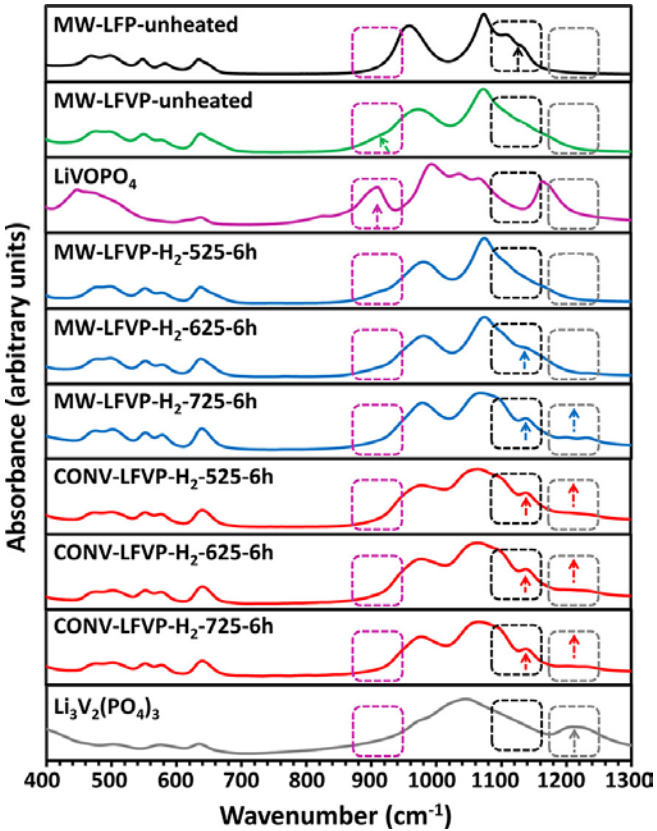

V^{3+} does not form a V=O bond so the shoulder around 900 cm^{-1} is not V=O.

FTIR shows no evidence of the "V=O" shoulder feature in any of the heated samples.

New peaks arise upon heating that are consistent with $Li_3V_2(PO_4)_3$.

Harrison, Bridges, Paranthaman, Segre, Katsoudas, Maroni, Idrobo, Goodenough, and Manthiram, 2013. *Chemistry of Materials*, 25(5), pp.768-781.

General XRD refinement details (Fullprof)

~ 10 wt.% Si in all XRD samples as internal standard.

Si spectrum refined first to obtain the lattice parameters and then the known Si lattice parameters were used in all other spectra to fix the zero position before refining battery materials.

The atomic displacement parameters were generally reasonable without any constraints (with a few exceptions), and it was generally possible to refine W, V, Y, and U for the olivine phase in most files (with the exception of U for a few samples).

- Y is a Lorentzian shape (half-width) parameter used with the "Thompson-Cox-Hastings pseudo-Voigt with axial divergence asymmetry" peak shape function in Fullprof.

It was difficult to refine $Li_3V_2(PO_4)_3$ because of low quantities so a pure $Li_3V_2(PO_4)_3$ sample was first refined and all of the parameters from that refinement were used for the $Li_3V_2(PO_4)_3$ impurity (only lattice parameters and the overall isotropic displacement parameter were refined for the $Li_3V_2(PO_4)_3$ phase in the olivine samples).

Harrison, Bridges, Paranthaman, Segre, Katsoudas, Maroni, Idrobo, Goodenough, and Manthiram, 2013. *Chemistry of Materials*, 25(5), pp.768-781.

XRD refinement assumptions (Fullprof)

Olivine refinement was based on assumption that all V was present on the Fe site.

- When V was allowed on Li site and total charge on Li site was restrained to 1^+, very high isotropic displacement parameters (Biso ~ 8) obtained, indicating likely non-physical results.
- Therefore, refinement not significantly improved by V on Li site and assuming that charge is balanced, supporting the assumption that there is not significant V doping on the Li site.
- However, restraining the total charge on the Li site to 1+ or the total charge on the Fe site to 2+ are just two possibilities!
- It is also possible that the charge is not perfectly balanced on each site as is the case when there are anti-site defects in $LiFePO_4$.

A restraint was placed on the Fe site such that the total charge had to be equal to 2^+ (assuming Fe^{2+} and $V^{3.2+}$ for pristine samples and V^{3+} for heated samples).

- V^{3+} yields reasonable results that converge and does not change the V occupancy within error.

The assumption that V is mostly substituted for Fe is consistent with ICP and the formation of impurities when other stoichiometries are assumed, but a small amount of V may be on Li site.

Harrison, Bridges, Paranthaman, Segre, Katsoudas, Maroni, Idrobo, Goodenough, and Manthiram, 2013. *Chemistry of Materials*, 25(5), pp.768-781.

General ND refinement details (GSAS and Fullprof)

^{7}Li enriched LiOH used for MW-ST synthesis samples refined by ND to decrease uncertainty in neutron scattering length because the ^{6}Li content can vary between sources.

ND not sensitive to V so V occupancy assumed on Fe site with V^{3+} and yields reasonably results.

- Attempts to refine with V^{4+} yielded non-physical results.

ND suggests slight Li deficiency, which is consistent with some V^{4+} as charge balance.

- Attempts to refine with V^{4+} yielded non-physical results.
- Attempts to refine Fe on the Li site yielded 0% Fe.
- Small amounts of V on the Li site might be possible but ND not sensitive enough to V to check.
- Small amounts of V doping on the Li site have been shown in the literature but lattice parameters should increase from that scenario (contrary to our results).
- ICP, lattice parameter changes, and observed impurities when varying precursor ratios suggest the bulk of the V doping occurs on Fe site.
- High doping on the Li site would also lead to large capacity losses that are not observed.

Harrison, Bridges, Paranthaman, Segre, Katsoudas, Maroni, Idrobo, Goodenough, and Manthiram, 2013. *Chemistry of Materials*, 25(5), pp.768-781.

Challenges we overcame…

- What if Li peaks are too weak?
  - Deposited thick Li layers (100-200 μm)
- What if Li sample is not flat?
  - Optimized sample preparation to be as flat as possible and use only data for strain where χ tilt < 55° to avoid beam elongation
- What if Be and/or Cu peaks overlap with Li?
  - Ran controls with LaB_6 and Cu substrate material with/without Be first
- How can the sample be positioned if the laser can be used for z height adjustment?
  - Pre-align holder with mock up sample and keep track of position
  - Perform final height adjustment with Li peak on actual film sample

Rodriguez, Harrison, Goriparti, Griego, Boyce, and Perdue, 2020. Powder Diffraction, 35(2), pp.89-97.

LaB_6 powder tested as a standard to check alignment shows near zero strain (this strain was offset from all other data)

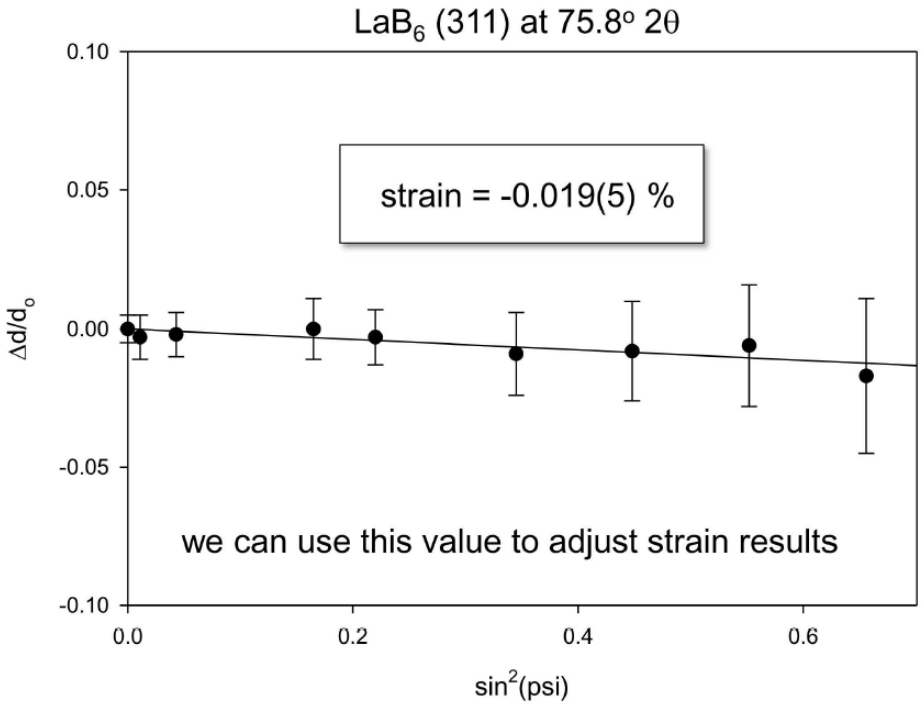

Rodriguez, Harrison, Goriparti, Griego, Boyce, and Perdue, 2020. Powder Diffraction, 35(2), pp.89-97.

Cu foil in Be dome tested as a standard to understand interference positions is essentially unstrained

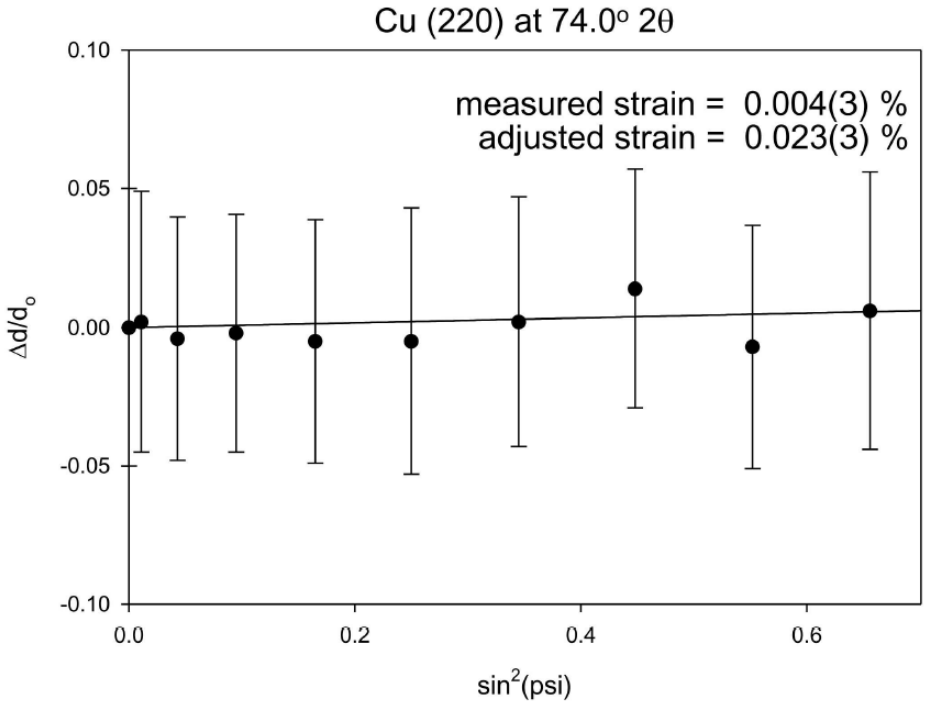

Rodriguez, Harrison, Goriparti, Griego, Boyce, and Perdue, 2020. Powder Diffraction, 35(2), pp.89-97.

Geometry and definition of XRD diffractometer angles

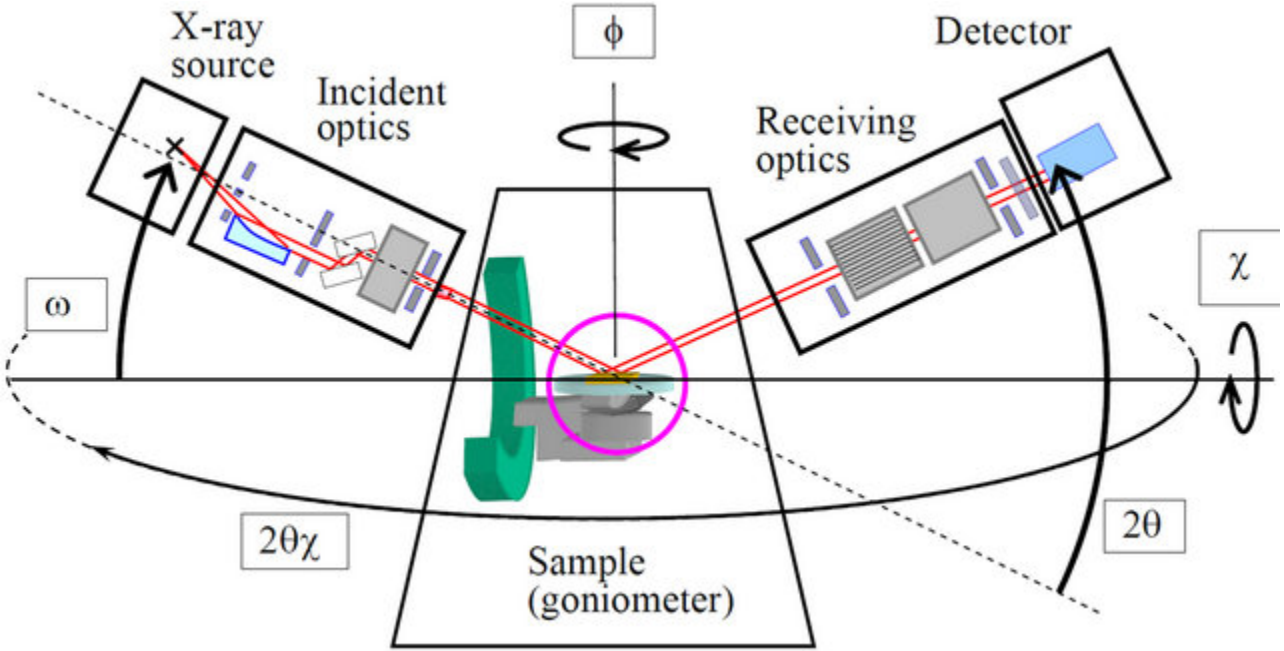

Inaba, K., Kobayashi, S., Uehara, K., Okada, A., Reddy, S.L. and Endo, T., 2013. High resolution X-ray diffraction analyses of (La, Sr) MnO 3/ZnO/Sapphire (0001) double heteroepitaxial films.

Li cycling leads to shredding of the current collector. How can a soft metal do that?

(a) Pristine
(b) 1ST plating
(c) 1st stripping
(d) 11th plating
(e) 51st plating
(f) 101st plating

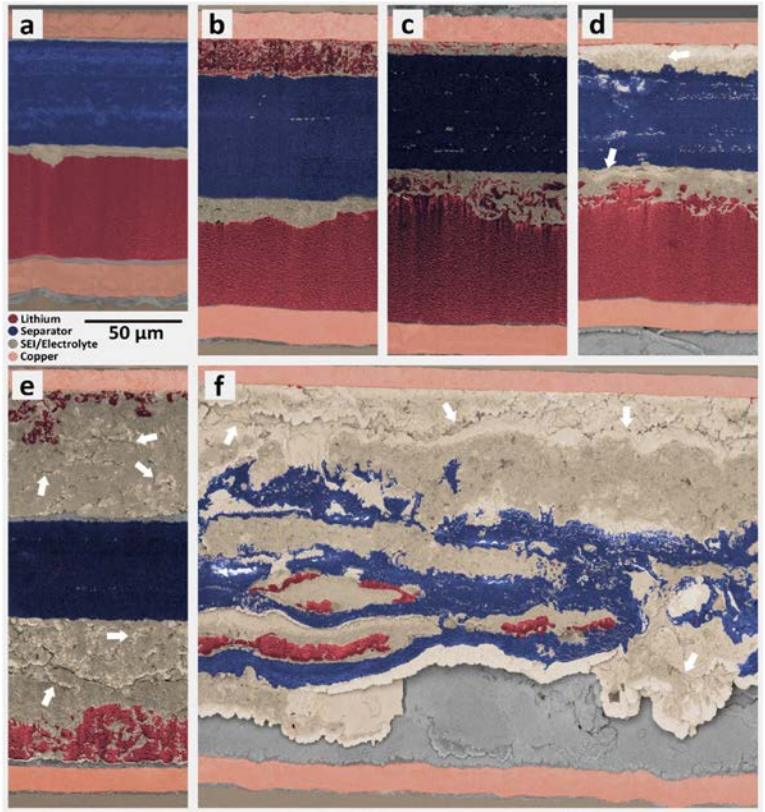

Jungjohann, Gannon, Goriparti, Randolph, Merrill, Johnson, Zavadil, Harris, and Harrison, 2021. *ACS Energy Letters*, *6*(6), pp.2138-2144.

Applied pressure improves morphology at low current

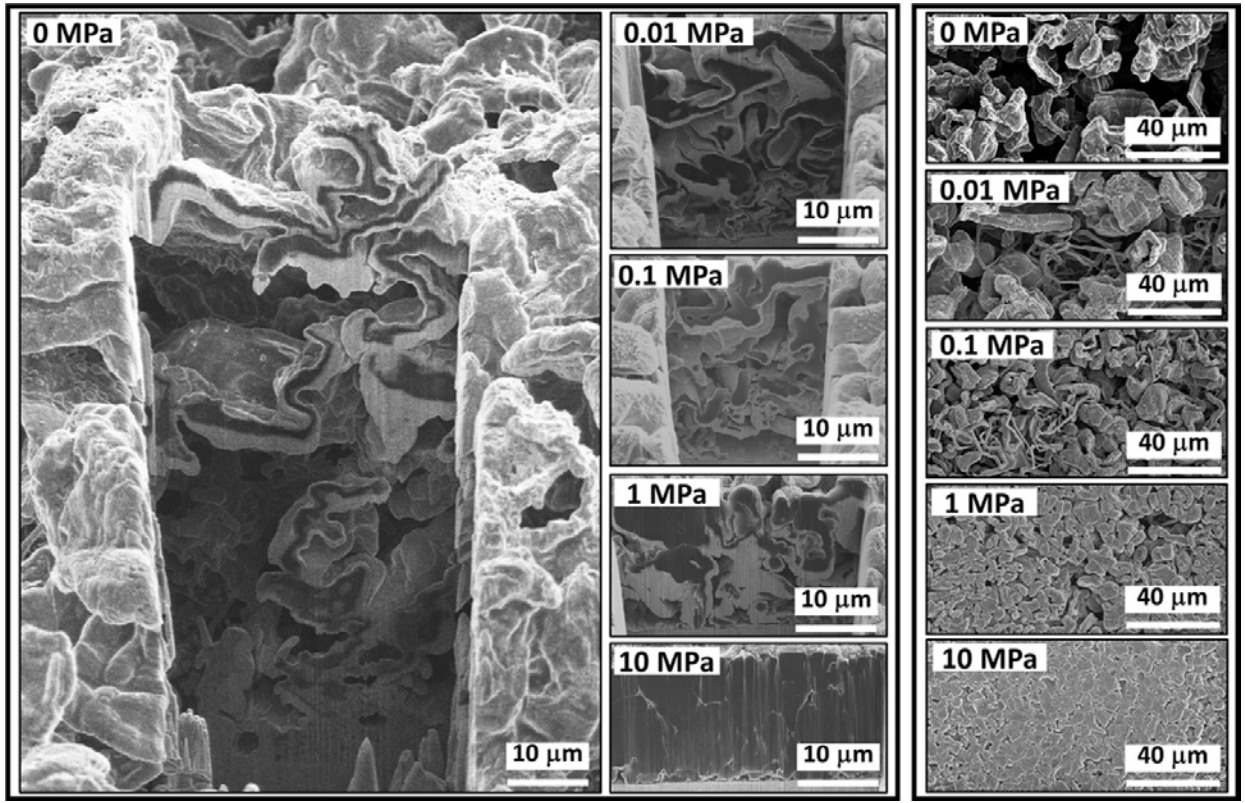

Harrison, Goriparti, Merrill, Long, Warren, Roberts, Perdue, Casias, Cuillier, Boyce, and Jungjohann, 2021. *ACS Applied Materials & Interfaces*, *13*(27), pp.31668-31679.

Applied pressure improves cycling at low to moderate pressures but too much pressure causes short circuits

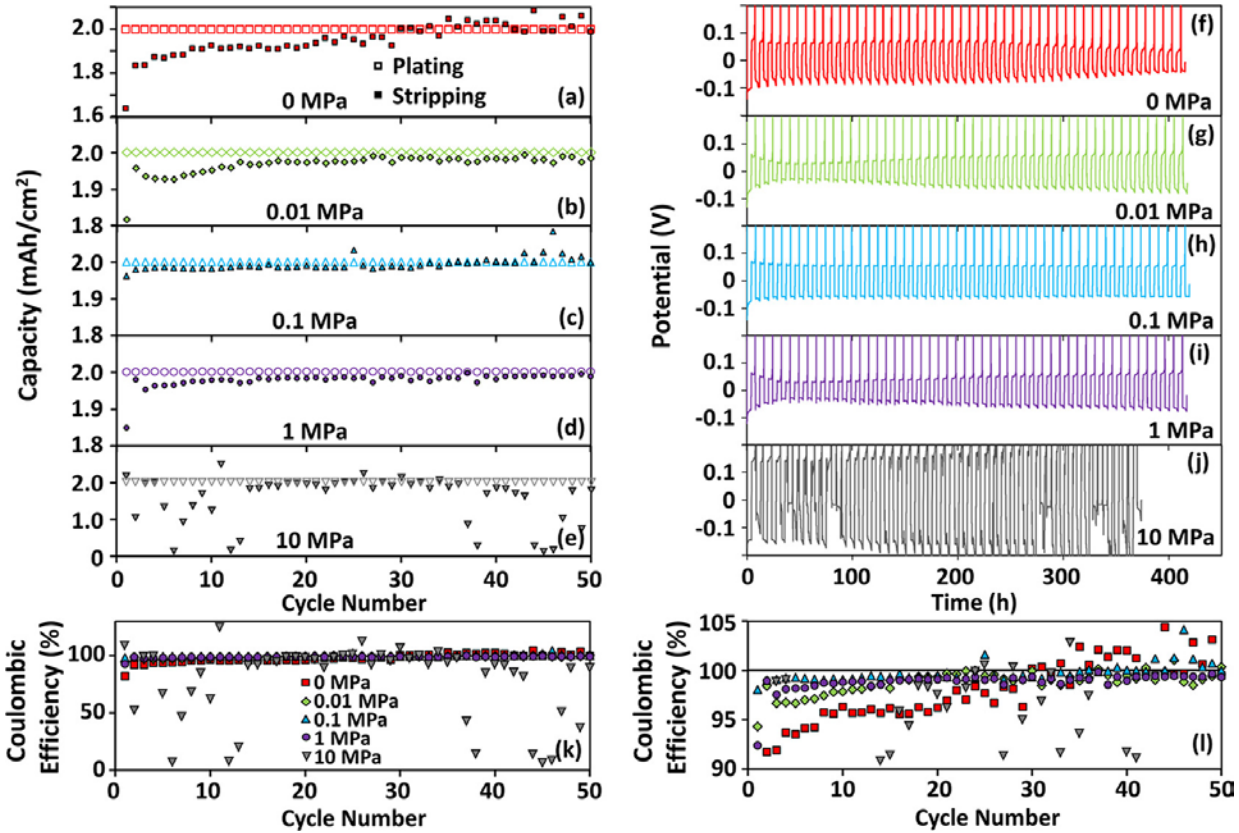

Harrison, Goriparti, Merrill, Long, Warren, Roberts, Perdue, Casias, Cuillier, Boyce, and Jungjohann, 2021. *ACS Applied Materials & Interfaces*, *13*(27), pp.31668-31679.

Morphology not super different at varied pressure for Li electrodeposited at high current

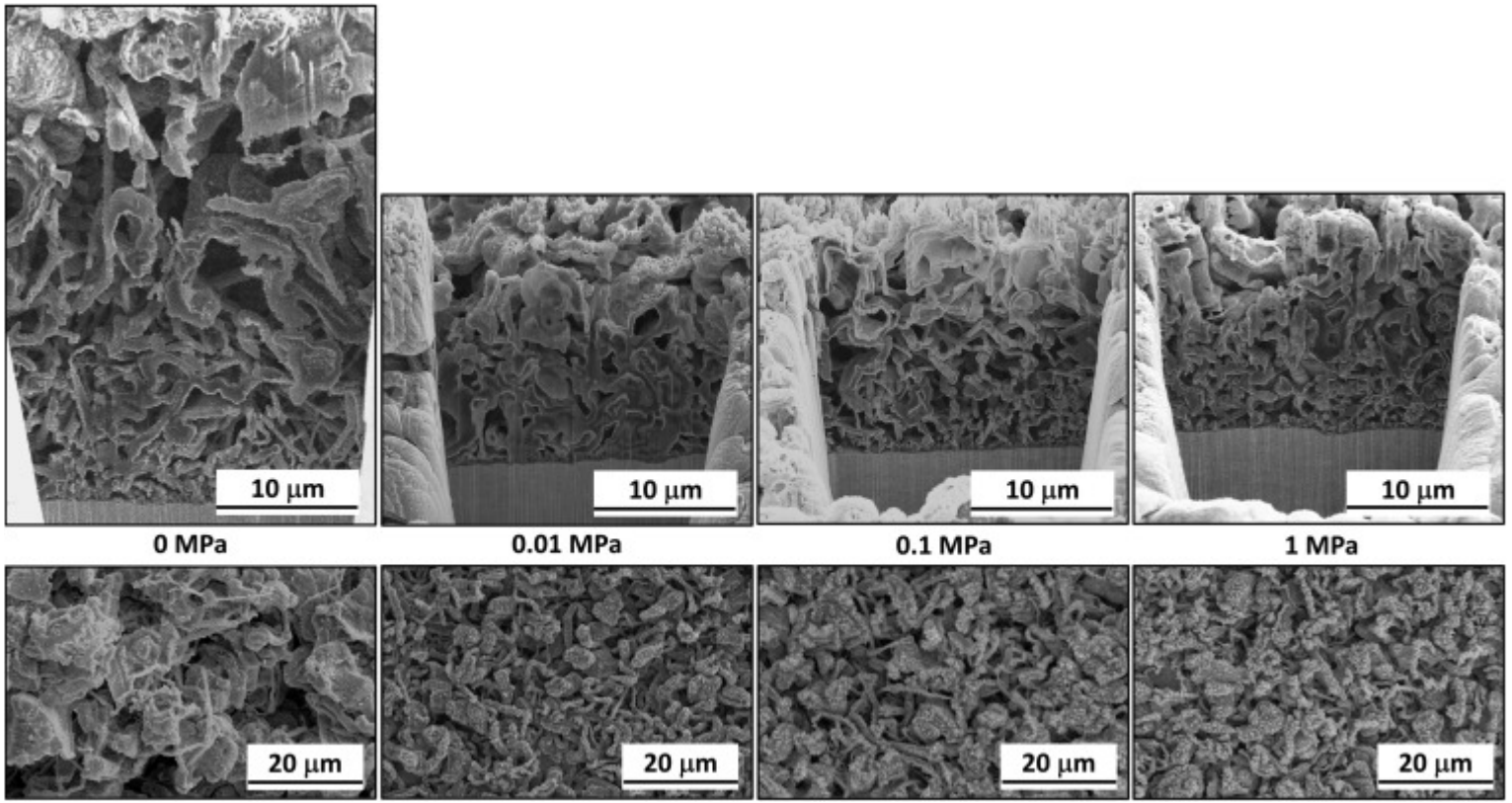

Harrison, Merrill, Long, Randolph, Goriparti, Christian, Warren, Roberts, Harris, Perry, and Jungjohann, 2021. *Iscience*, *24*(12).

Li grows through separators after 50 cycles at all pressures

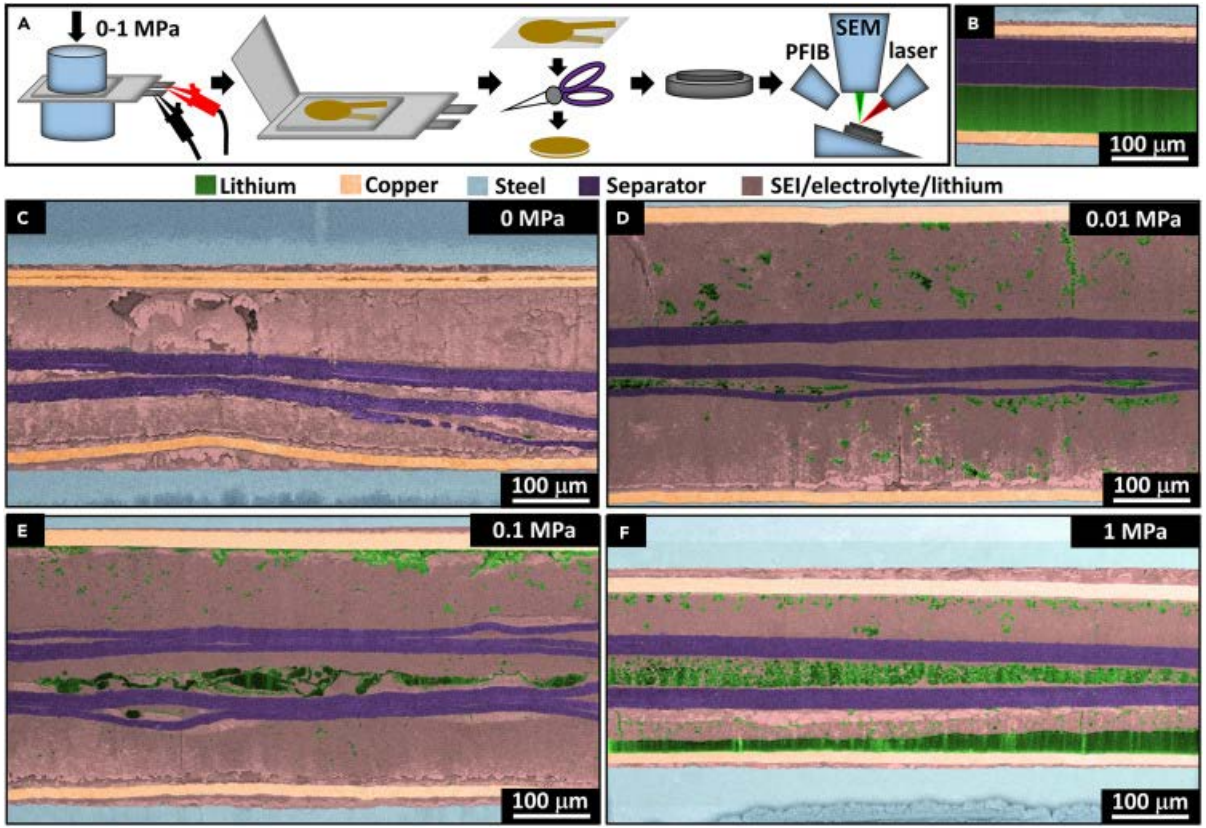

Harrison, Merrill, Long, Randolph, Goriparti, Christian, Warren, Roberts, Harris, Perry, and Jungjohann, 2021. *Iscience*, *24*(12).

Pressure causes more evidence of short circuits at high current density

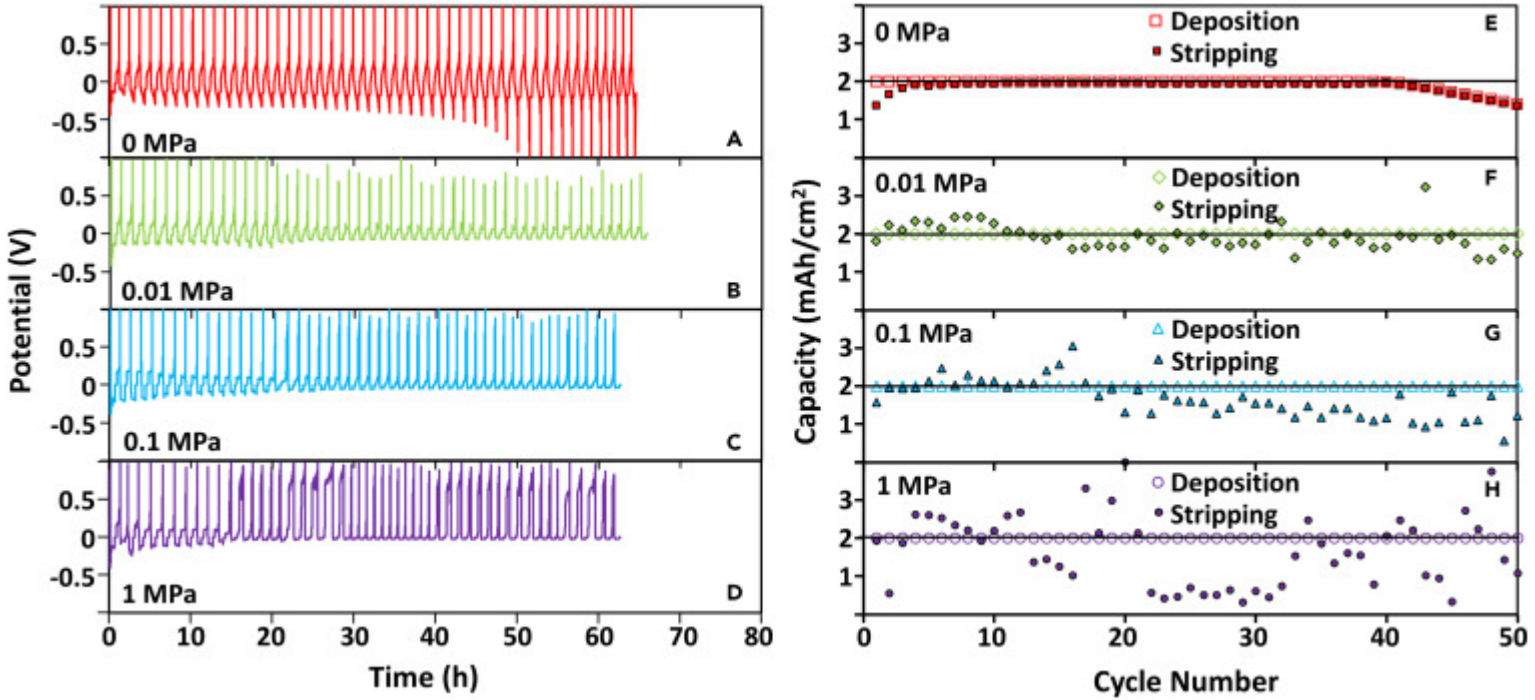

Harrison, Merrill, Long, Randolph, Goriparti, Christian, Warren, Roberts, Harris, Perry, and Jungjohann, 2021. *Iscience*, *24*(12).

Impedance after various cycles with various pressures and 1 versus 2 separators at high current density

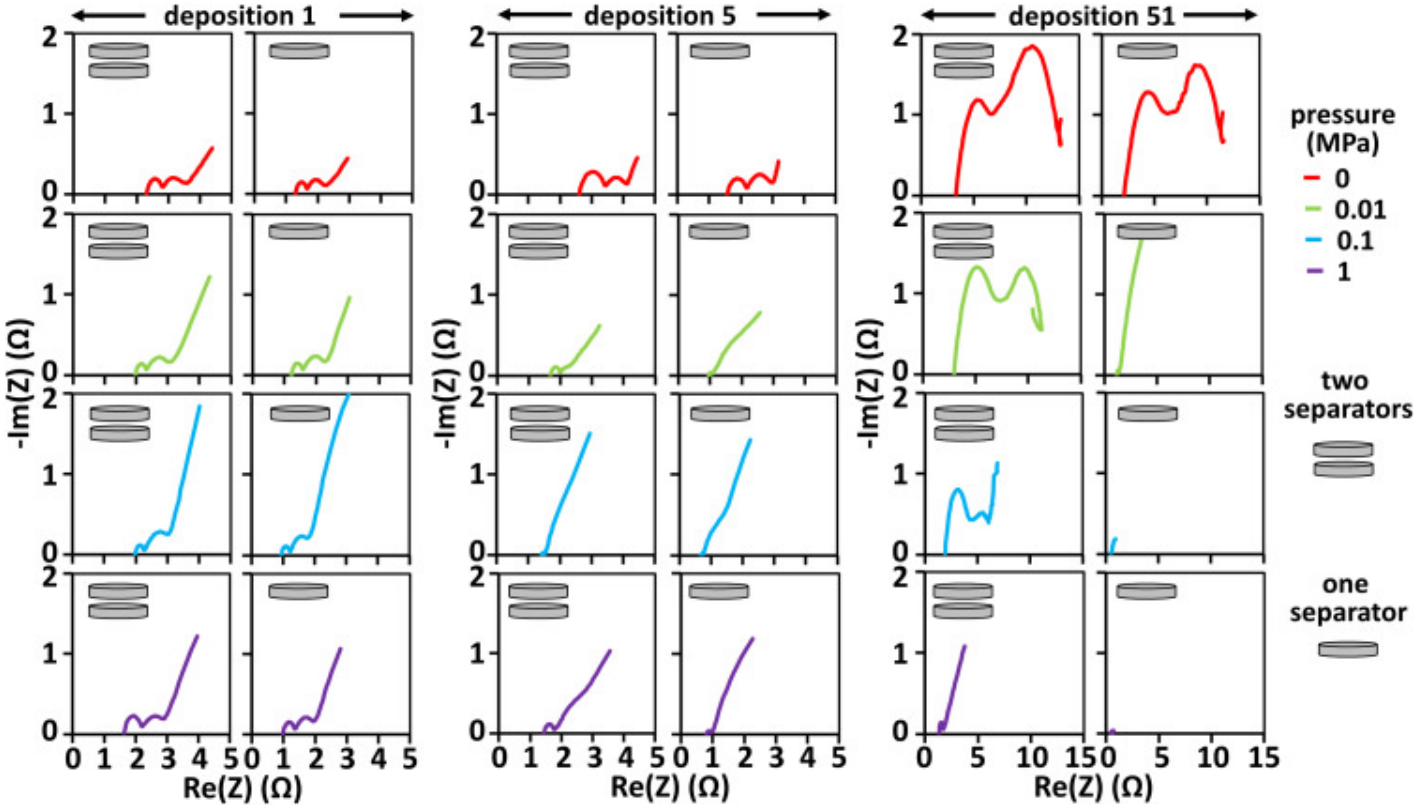

Harrison, Merrill, Long, Randolph, Goriparti, Christian, Warren, Roberts, Harris, Perry, and Jungjohann, 2021. *Iscience*, *24*(12).